ADVANCES IN PHYSICS, 2001, VOL. 50, NO. 3, 297–341

Issues in the statistical mechanics of steady sedimentation

SRIRAM RAMASWAMY*
Centre for Condensed-Matter Theory,
Department of Physics, Indian Institute of Science,
Bangalore 560 012, India

[Received 22 September 2000; accepted 16 March 2001]

Abstract

A critical review is presented of recent experimental and theoretical work on the steady sedimentation of particulate suspensions in viscous fluids. The point of view is that of a practitioner of non-equilibrium statistical physics rather than classical fluid mechanics.

Contents PAGE

* e-mail: sriram@ physics.iisc.ernet.in

Advances in Physics ISSN 0001–8732 print/ISSN 1460–6976 online
http://www.tandf.co.uk/journals
DOI: 10.1080/0001873011005061 7

1. Introduction

1.1. *Equilibrium and non-equilibrium suspensions*

Suspension science and statistical physics have a long and distinguished common history, beginning with the classic theoretical [1–4] and experimental [5] studies of Brownian motion. These early works dealt primarily with suspensions at or near *thermal equilibrium*, which meant that the source of fluctuations in the systems considered is a thermal bath characterized by a temperature, and that correlation and response functions of physical observables are tightly linked by fluctuation–dissipation relations. The interest of physicists in the statistical mechanics and dynamics of suspensions [6, 7] has continued to the present day, with the focus shifting progressively to problems of systems far from equilibrium. The effect of shear flow on the structure and crystallization of suspensions has received a great deal of attention [8]; the conceptually simpler state of sedimentation [9–11], where there is on average no *relative* motion of the particles, is the subject of this article. I shall not say anything about the many practical situations in which sedimentation is important; some references to this can be found in reference [10], for instance.

1.1.1. *Driven suspensions and hydrodynamic dispersion*

I shall discuss recent progress, puzzles and controversies in *steadily sedimenting suspensions*. Such systems are in a *non-equilibrium steady state* and therefore have properties qualitatively different, in two important ways, from those of the thermal equilibrium suspensions mentioned above. First, they are *driven*, i.e. the particles in the suspension are denser than the fluid and, hence, have on the average a downward speed relative to it, as a result of the balance between gravity and viscous dissipation. Secondly, driven suspensions, whether sedimenting or sheared, display random particle motion even when the particles are so large that *thermal* Brownian motion is negligible: the flow produced by each particle influences the others in such a way that the dynamics is highly sensitive to initial conditions. The resulting chaos [12, 13] implies that the time-evolution of coarse-grained quantities must be described using diffusion coefficients and noise sources even though the microscopic dynamics in

the absence of thermal Brownian motion is entirely deterministic. This phenomenon of diffusive behaviour induced, in the absence of a thermal noise, by the flows generated by the collection of objects driven through a fluid is called *hydrodynamic diffusion* or *hydrodynamic dispersion*. This places all questions about the large-scale structure and long-time dynamics of sedimenting or sheared suspensions squarely in the domain of *non-equilibrium statistical physics* rather than traditional fluid dynamics.

In general, the particles of a suspension are acted upon by Brownian and other forces. If D_{th} is the *thermal, Brownian* diffusivity of a solute particle of radius a, in a flow with typical velocity gradient $\dot{\gamma}$ around the particle, the *Péclet number*

$$\mathrm{Pe} = \frac{\dot{\gamma} a^2}{D_{\mathrm{th}}} \tag{1}$$

is a dimensionless measure of the relative importance of flow and thermal diffusion in the suspension. For a particle moving (for example, sedimenting) at speed v through an unbounded fluid, $\dot{\gamma} \sim v/a$, so that

$$\mathrm{Pe} = \frac{va}{D_{\mathrm{th}}}. \tag{2}$$

For a Brownian sphere of radius a and buoyant weight (i.e. weight minus the weight of solvent displaced) $W \equiv m_{\mathrm{R}} g$, where g is the acceleration due to gravity, settling through a viscous fluid at temperature $k_{\mathrm{B}}T$ in energy units, the settling speed $v = m_{\mathrm{R}} g/\Gamma$, where Γ is the coefficient of viscous drag on the fluid and the Einstein relation tells us that the diffusivity $D_{\mathrm{th}} = k_{\mathrm{B}}T/\Gamma$. Thus $\mathrm{Pe} = m_{\mathrm{R}} ga/k_{\mathrm{B}}T$ irrespective of the detailed relation between Γ and the fluid viscosity. In this form the Péclet number is seen to be simply the effective gravitational potential energy difference across a height equal to the particle size, scaled by the temperature; curiously, it is independent of the kinetic coefficients of the system.

We shall call a suspension in which Pe is exceedingly large, say 10^2 or more, a *non-Brownian* suspension. In such suspensions the physics is dominated by the interplay of the driving force (gravity in the case of sedimentation) and hydrodynamics, with *thermal* fluctuations playing a negligible role. As in flowing powders, and in marked contrast to textbook [14] non-equilibrium steady states such as the flow of electrical or thermal currents, the scales of the fluctuations and hydrodynamic diffusivities in driven non-Brownian suspensions, and the very nature of their linear response about the driven state, are determined by the driving force. They have nothing to do with the thermodynamic temperature of the system and are hence not constrained by fluctuation–dissipation relations. Even in suspensions with $\mathrm{Pe} \sim 1$, there will be substantial non-equilibrium contributions to diffusion, fluctuations and linear response. These ideas will be seen to have profoundly important consequences for the nature of the dynamics and correlations in sedimenting suspensions.

1.2. *Crystalline and fluid-like suspensions*

As is well known [6], charge-stabilized as well as hard-sphere suspensions can crystallize at high enough particle volume fraction and low ionic strength of the solvent. I shall call such ordered systems *crystalline suspensions*, and those with a disordered microstructure with freely moving particles *fluid-like suspensions*. The latter are sometimes called *disordered suspensions*, but such a name is confusing

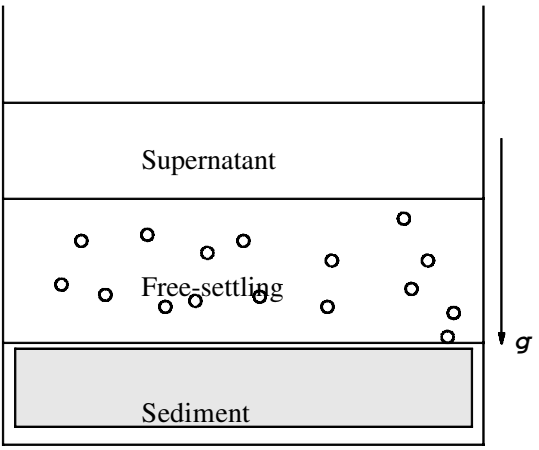

Figure 1. Sedimentation in the conventional batch settling geometry.

because it could equally be applied to amorphous but rigid aggregates. My choice of names is non-standard but clearer.

1.3. *Steady sedimentation and the fluidized bed geometry*

This article is not directly concerned with the most familiar aspect of sedimentation, namely, the separation (see figure 1), of a suspension into sediment and supernatant, with a free-settling layer in between [9], but exclusively with *steady sedimentation*. This state can in principle be realized by studying the free-settling region alone, while feeding particles in from the top to compensate for those that go into the sediment. A particularly elegant way of achieving this ideal, spatially homogeneous, perpetually settling state is to comove with the settling particles, in the 'fluidized bed' geometry (see, for example, reference [15]) as follows. Subject the suspension to an upward flow of speed v_0 from below (figure 2). The system will choose a constant, spatially uniform number density n_0 compatible with this flow rate. For samples whose linear dimensions are large in all directions, the behaviour, apart from a change of reference frame, should then be identical in the bulk to that of a collection of particles with number density n_0 settling with speed v_0 in the laboratory frame in an unbounded fluid. Although not all experiments attempting to probe the statistical properties of steady-state sedimentation are performed in the fluidized-bed geometry, it is the ideal setting for such studies. All the experiments I shall discuss in this article, even those performed in conventional batch sedimentation, are carried out under the implicit assumption that the underlying state is statistically stationary. Throughout this article I shall be concerned only with the nature of such a steadily sedimenting state and fluctuations about this state.

1.4. *Low Reynolds number flow*

The Reynolds number $\mathrm{Re} \equiv UL\rho/\mu$ measures the ratio of inertial to viscous forces in the flow of a fluid with shear viscosity μ and mass density ρ, with typical scales U and L of velocity and length respectively. For the suspensions with which this article is concerned, Re ranges from 10^{-6} if L is a particle size up to 10^{-4} if we take L to be the interparticle distance. Except for a very brief diversion at

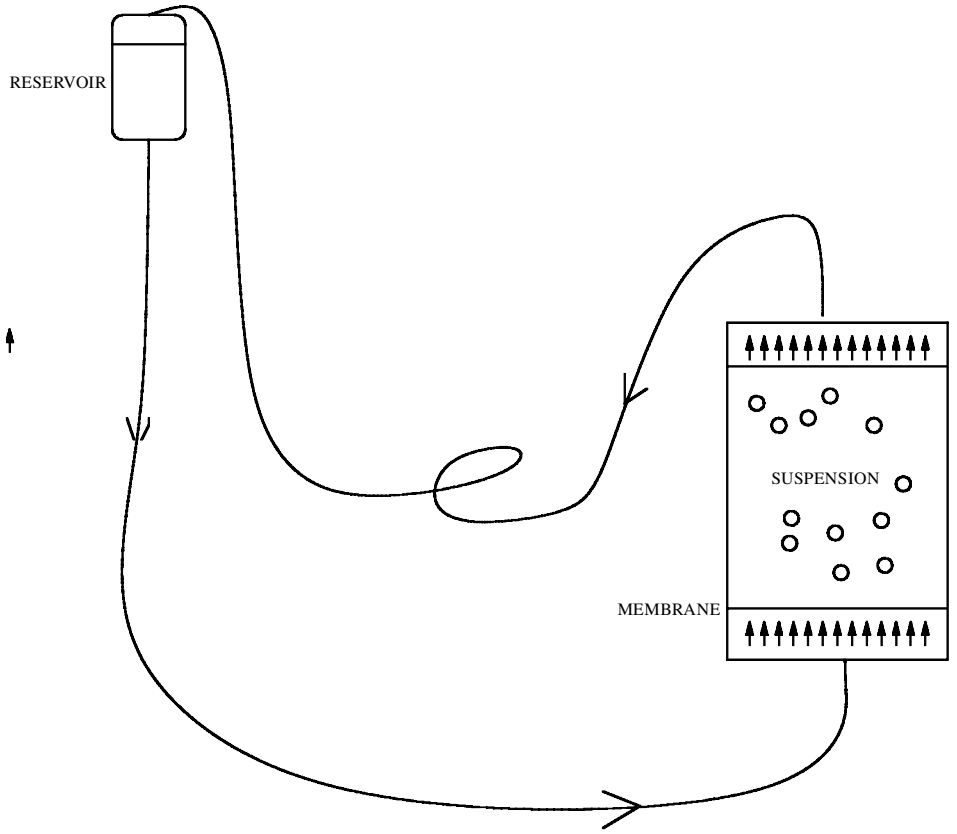

Figure 2. Schematic diagram of a fluidized bed. The viscous drag of a fluid flow imposed from below balances the Archimedean weight of the particles, suspending them stably on average. The flow rate is sustained by a pressure reservoir, made uniform by a membrane diffuser, and measured by the outflow through the top.

the end of section 4, I shall therefore work in the *Stokesian* limit $\mathrm{Re} = 0$ throughout this article.

Several important features of Stokesian flow in the presence of particles [9] are summarized here. (i) The equations of fluid flow in this limit are *linear*. (ii) An isolated single particle of buoyant weight W settling under gravity in an unbounded container gives rise to a velocity field decaying as W/r with distance r from the particle. (iii) A localized density fluctuation about a background of uniform concentration of settling particles likewise produces a $1/r$ velocity fluctuation. (iv) The relative velocity of an isolated pair of settling particles in an unbounded fluid is zero: they neither approach nor recede from nor rotate about each other. If they start out at the same height, they fall together (figure 3(*a*)), at a speed greater than that of an isolated single particle subjected to the same force. If they are initially separated both vertically and horizontally, their centre of mass falls not vertically but obliquely, the velocity pointing in a direction between the vertical and the vector joining the higher particle to the lower (figure 3(*b*)). (v) The dynamics of three or more particles is complex and chaotic [13].

The remainder of this article is organized as follows. Section 2 gives a synoptic view of the problems of interest here and the progress that has been made. Section 3

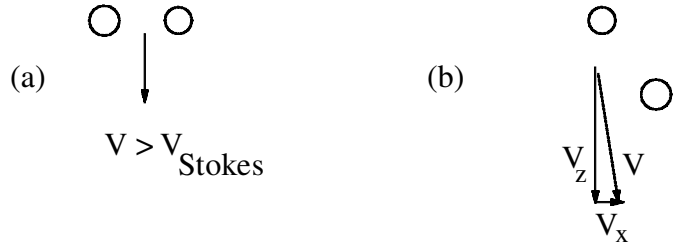

Figure 3. (*a*) A pair of particles settling side by side settles faster than an isolated particle; (*b*) a pair with oblique separation vector settles with a small horizontal component to its velocity.

is a reminder of the essentials of fluid dynamics as applied to slow sedimentation. Section 4 treats the problem of velocity fluctuations in monodisperse hard-sphere sedimentation. In section 5 I discuss crystalline fluidized beds. Section 6 summarizes our understanding of the statistical physics of bidisperse sedimentation, and the review closes with section 7.

2. Scope of this article

The physics problems posed by sedimentation are not familiar even to many workers in soft-matter science or statistical mechanics. This section therefore is a short synopsis to acquaint the reader with the major questions with which this article is concerned. It should also serve as a precis, for the reader who does not want the detail of the sections that follow.

This article focuses on three classes of ***fluctuation*** phenomena in sedimentation, with reference to experiments on model, size-controlled suspensions of synthetic particles. These are: (i) the nature of velocity fluctuations in viscous fluidized beds of monodisperse hard spheres; (ii) the instability of steadily sedimenting lattices; and (iii) the competition between depletion and hydrodynamic forces in bidisperse sedimentation. Questions about the mean settling speed of various ordered or disordered configurations of particles, which form a large part of the sedimentation literature, are not the main concern of this review, although I shall discuss them briefly to highlight the long-ranged nature of the hydrodynamic interaction. In addition, this article is on the *collective* statistical properties of sedimenting suspensions, not the *derivation* of their stochastic behaviour from N-body Stokesian dynamics. My discussion (section 3.4) of the microscopic origin of hydrodynamic dispersion (see section 1.1.1) will therefore be very brief.

Apart from highlighting recent advances in the field and presenting open problems, this survey aims to convince theoreticians and experimenters alike that the old subject of suspension dynamics poses exciting problems at the frontiers of non-equilibrium statistical physics. It will become clear, in particular, that techniques originally developed to understand the dynamics of critical point and related phenomena at thermal equilibrium are an essential tool in building systematic theories of these driven systems.

Important progress has been made on each of the three problems mentioned above, in both experiment and theory. At the same time, several puzzles remain, as do diverging views on basic issues. Let me define each problem first and outline the progress made.

2.1. *Velocity fluctuations in hard-sphere sedimentation*

2.1.1. *Caflisch and Luke's puzzle*

A major surprise in the statistical physics of sedimentation was pointed out by Caflisch and Luke (hereafter CL) [16]. Let me restate it very briefly here, following Segrè *et al*. [17] and Hinch [18]. Consider a steadily sedimenting fluid-like suspension (see section 1.3) of hard spheres. A concentration *fluctuation* near, say, the origin in this suspension is a pointlike force density and should, as mentioned in section 1.4, give rise in three space dimensions to a velocity *fluctuation* decaying as $1/r$ with distance r from the origin. The linearity of Stokes flow implies that the velocity field resulting from many, spatially distributed concentration fluctuations is simply the sum $\sum_i v_i$ of the individual contributions. If these fluctuations take place in a random, *spatially uncorrelated* manner throughout the suspension, the resulting variance σ_v^2 in the velocity at any point in the suspension would clearly be the sum of the squares of the individual contributions. This sum $\sum v_i^2$ has $N \sim L^3$ terms if there are N solute particles in a container of linear dimension L in all directions. The $1/r$ form mentioned above for the velocity fluctuation produced by a localized concentration fluctuation means that each term $\langle v_i^2 \rangle \sim L^{-2}$, so that $\sigma_v^2 \sim L$. Such a diverging variance in the infinite-L limit poses serious problems for calculations [19] of the mean settling speed in an unbounded suspension.

Most experiments† find no size dependence of the sort predicted by Caflisch and Luke, but there are serious questions [21] that can be asked about the interpretation of the measurements. It is fair to say that experiments have neither confirmed the CL predictions nor definitely ruled them out. It should of course be noted that CL's 'prediction' said only that *if* the concentration fluctuations were statistically independent from one point to another in space then the velocity variance must diverge. Sufficiently strong *anticorrelations* in the particle concentration field at large length scales will suppress the CL divergence (see section 4.2). Clearly what is needed is a theory that tackles concentration and velocity fluctuations on the same footing, instead of postulating the one and inferring the other. Let me summarize the theoretical approaches to this problem after a very short description of the experiments.

2.1.2. *Experiments and simulations in brief*

Experiments on the velocity-fluctuations problem use a wide range of techniques including tracking the velocity field by particle imaging [17], direct counting of the particles in an illuminated region [20, 22], diffusing-wave spectroscopy [15], tracking the motion of individual 'tagged' particles in a suspension of otherwise index-matched spheres [20, 23–25] and single, as well as multiple, *sound*-scattering [26]. It has generally been claimed [17, 25], with one significant exception [20], that the fluctuations saturate to a size-independent value, but this interpretation has been criticized [21]. Numerical simulations [27] saw clear evidence for the size-dependence over the range of L explored, although it is argued [17] that this was because these studies were probing scales smaller than a (large) screening length. We shall return to a more detailed consideration of these issues in section 4.3.

† Tory (see reference [20] and work cited therein) argues strongly in favour of size-dependent velocity fluctuations.

There is also a class of experiments [28] which separates the problem of hydrodynamic diffusion and non-equilibrium statistical behaviour in fluidized beds from the question of whether the velocity variance diverges. This it accomplishes by working with a suspension in an effectively two-dimensional geometry, i.e. with length L and width W much larger than the thickness δ, and δ only slightly larger than the particle size. This yields a system whose local hydrodynamics is three-dimensional, so that hydrodynamic dispersion does take place, but with long-range effects including any possible Caflisch–Luke divergence screened out on lateral scales $\gg \delta$. The measurements of the probability distribution of velocity fluctuations and hyperdiffusive particle in these experiments still lack a theory. The work of Xue *et al.* [15] using diffusing-wave spectroscopy and the particle-imaging velocimetry of Segrè *et al.* [29] also fall broadly into this category. Since these interesting and important experiments do not specifically concern themselves with the question of the divergent velocity variance, I shall not discuss them here. The confined experimental geometry, however, is of particular relevance to the content of section 5, and the notion [29] of an effective temperature is central to the stochastic PDE approach of reference [30].

2.1.3. *Theoretical approaches: a summary*

Apart from ideas involving particle or fluid inertia†, which experiments [26] seem to have ruled out pretty conclusively, there are precisely four theoretical attempts to go beyond what Caflisch and Luke (CL) did. Koch and Shaqfeh (KS) [31] were the first to argue that a mechanism analogous to screening of the Coulomb interaction in electrolytes might be at work in sedimenting suspensions. They start from a microscopic statistical description of the interaction of sedimenting, hydrodynamically interacting particles and show that considerations involving three-particle encounters could lead to a screening of the CL divergence. They do not, however, suggest independent measurements which could predict whether a given suspension will be screened. Brenner [21] assumes the CL mechanism but questions the claimed evidence in favour of screening, arguing that the interpretation of the experiments [17] which attempted to test it are greatly complicated by the proximate walls of the container. The coarse-grained approach of Levine *et al.* [30] consists of writing down stochastic equations of motion for the concentration and velocity fields of a sedimenting suspension, retaining only those terms which dominate at large length scales, and assuming no relations amongst the phenomenological parameters other than those forced on one by the symmetries of the problem. The spirit is identical to that underlying theories of dynamical critical phenomena [32], the hydrodynamics of ordered phases [33], or indeed the fluctuating Navier–Stokes equations [34]. The important difference is that sedimentation is a *non-equilibrium* steady state, so that the stationary configuration probabilities are not given by a Boltzmann–Gibbs distribution with respect to an energy function, but must be obtained by solving the equations of motion. This approach actually yields a phase diagram for steady sedimentation, containing an 'unscreened' phase in which the velocity variance σ_v^2 diverges as L, as in CL, and a 'screened' phase in which σ_v^2 saturates for L greater than a *screening length* ξ. Lastly, Tong and Ackerson [35] make the intriguing observation that the model equations for sedimentation at large Pe number and

† Brenner [21] suggests a role for inertia in producing one kind of screening in sedimentation.

small Reynolds number are identical to those for *thermal* convection at large Prandtl and Rayleigh numbers, with the concentration in the sedimentation problem standing in for the temperature field in the convection problem. They then transcribe results from Kraichnan's mixing-length theory for Rayleigh–Bénard turbulence to argue for screening and, hence, for a finite velocity variance in steady, low Reynolds-number sedimentation. The analogy is tantalizingly close and, although their paper presents no detailed calculations, I suspect it contains a great deal of the essential physics. An important difference between reference [35] and the experiments is that the latter are done with a uniform concentration whereas convection is driven by an imposed temperature gradient. Tong and Ackerson's work and that of Levine *et al.* [30] are, I believe, equivalent, although the former is a set of highly plausible physical arguments while the latter is a detailed calculation within a phenomenological theory. My review will discuss all of the above theoretical approaches in some detail.

2.2. *Sedimenting crystalline suspensions*

If the mass densities of solute particles and solvent are matched, there is no sedimentation. Such a *neutrally buoyant* suspension of monodisperse spheres is a scale model for a classical liquid at thermal equilibrium insofar as its static structural properties are concerned [6]. As the particle volume fraction ϕ and, in the case of charge-stabilized suspensions, the Debye screening length $\xi_D \equiv \kappa^{-1}$ are increased, the spatial correlations in the positions of the suspended particles change from gas-like, through liquid-like, finally to crystalline. The lattice spacing in the crystalline phase is generally of the order of microns or larger for the cases of interest. The term *colloidal crystals* is often applied to crystalline suspensions, even when the particle size is large. The phase diagrams of these systems are generally studied by changing not the temperature but the ionic impurity strength n_i. A large n_i means a short ξ_D and hence a weaker interaction. Temperature itself is not a convenient parameter to vary: the dielectric constant of water makes the combination (interaction energy/temperature) rather weakly dependent on temperature. These suspensions have a phase diagram which is well understood at thermal equilibrium [6], using methods taken from the theory of freezing of classical liquids [36].

Recall, however, that the materials favoured in the making of synthetic colloids—polystyrene, specific gravity 1.05, and silica, specific gravity 2—are heavier than water. Left to itself, a crystalline aqueous suspension made of such particles will settle slowly, resulting in a slightly inhomogeneous, bottom-heavy crystal with unit cells shorter at the lower end of the container than at the top. For very small polymer particles (say polystyrene spheres, specific gravity 1.05, 0.1 μm in diameter) the effect is negligible except on enormous time scales. For larger, denser particles (e.g. 0.3 μm diameter silica spheres, specific gravity 2.5) the effect begins to be appreciable (Pe $\simeq 0.2$), and for spheres several microns in size it dominates. From the point of view of this review, this density mismatch offers the opportunity to study the structure and dynamics of a deformable lattice being driven uniformly through a viscous medium. A fluidized-bed experiment on a colloidal crystal [37, 38] will therefore allow us to examine in detail the steady-state properties of this process. A non-equilibrium steady state of this type also arises when a depinned flux lattice drifts under the action of the Lorentz force of an imposed supercurrent through a type-II superconductor and our interest in the subject of drifting crystalline arrays arose from efforts to understand flux-lattice motion. Whereas the structure and motion of

flowing flux-lattices has been very widely studied [39], with particular emphasis on the effect of static obstacles (impurities or voids), the corresponding problem in the context of suspensions, where such 'quenched disorder' does not arise, has received relatively little attention. The mean sedimentation speed of ordered, rigid arrays of particles is well understood [19] but references [37, 38, 40–43] are to my knowledge the only papers on the statistical mechanics and the dynamics of perturbations of such lattices.

References [40, 41] regard the perfect crystal, drifting steadily through a dissipative medium, as a non-equilibrium ordered phase, and use symmetry arguments to construct its linear response, i.e. the dispersion relation between the frequency and the wavenumber of a small-amplitude, long-wavelength disturbance. For a crystal at *thermal equilibrium*, e.g. for a neutrally buoyant colloidal crystal or a flux lattice at rest, this response is of course determined completely by elastic theory [44] and its extension to time-dependent phenomena [33]. The analysis of references [40, 41] showed that the dominant linear response of the drifting crystal at sufficiently long wavelengths was determined not by the elastic constants of the lattice but by the dependence of its local mobility on the local state of distortion. The scale of the terms in the terms in the equations of motion that led to such a response was shown to be controlled by the driving force on the lattice.

Even more strikingly, it was found [40] that this linear response could be either restoring or destabilizing: a crystal drifting through a viscous medium could, if disturbed, display *either* propagating waves with a speed that had nothing to do with its elastic constants *or* exponentially growing distortions leading to a clumped and buckled state. Which of these happens cannot be determined by symmetry arguments, but requires a detailed consideration of the interactions in the system. Thus, the stability or otherwise of a steadily sedimenting colloidal crystal could be established only by starting with a collection of particles interacting, say electrostatically, so as to form a crystal when neutrally buoyant, then switching on sedimentation and introducing a weak, long-wavelength sinusoidal perturbation in the particle positions. The perturbation will result in disturbances in the hydrodynamic flow which will in turn further alter the particle positions. The question then is whether this results in a growing or a decaying perturbation. A first step towards answering that question was taken a long time ago by Crowley [43] who considered the dynamical stability of collections of hard spheres prepared in perfectly ordered one- or two-dimensional arrays sedimenting normal to the ordering direction(s) in a viscous fluid. He found, experimentally and theoretically, that these arrays were always unstable. His arrays, however, were simply prepared in an initially ordered configuration, and had no interactions that could stabilize such order in the absence of sedimentation. In addition, his analysis was linear, and did not take into account the possible effects of thermal or hydrodynamic noise. In references [40, 41], all of these shortcomings were overcome, albeit in a simplified one-dimensional model, and it was concluded that steadily sedimenting crystalline suspensions were always *linearly unstable* to long-wavelength clumping and buckling. The analogous calculation [45] for drifting flux lattices showed that the latter were linearly *stable* and carried wavelike excitations.

These studies gave rise to new models in the general class known as *driven diffusive lattice gases* [46], with important consequences for non-equilibrium statistical mechanics. They showed spontaneous phase separation and breaking of translation invariance in a one-dimensional system with local, bounded interactions,

and ultraslow coarsening—domain size growing as the logarithm of time. This latter is to be contrasted with the power-law growth almost universally [47] found for coarsening in systems without quenched disorder.

The vast literature on sedimentation and related phenomena has little to say about the admittedly academic subject of crystalline fluidized beds. The only detailed experimental study on the subject [37, 38], although not a test of the predictions of references [40, 41], suggests that crystalline fluidized beds are indeed unstable, at least when their elasticity is weak. Further experiments, designed specifically to test the ideas of references [40, 41] are needed before one can claim to have understood the statistical mechanics of steadily sedimenting crystalline suspensions.

2.3. *Bidisperse sedimentation*

2.3.1. *Bidispersity and the depletion force*

Suspensions in nature and industry generally contain mixtures of particles of different types, shapes and sizes [48]. The simplest example of such polydispersity is found in a *bidisperse* suspension of chemically identical hard spheres of two different radii a_1 and $a_2 < a_1$. The *equilibrium* statistical physics of *Brownian*, *neutrally buoyant*, bidisperse hard-sphere mixtures is fairly well understood [49, 50]. Asakura and Oosawa [49] made the crucial observation that a pair of large hard spheres in a bath of smaller spheres would attract each other if they got close enough such that there was no room for a small sphere to fit between them (figure 4). This *depletion interaction* can be seen as arising from the unbalanced pressure because the small-sphere gas does not have access to part of the large-sphere surfaces, or equivalently by noting that moving the large spheres together increases the available volume for, and hence the entropy of, the small spheres.

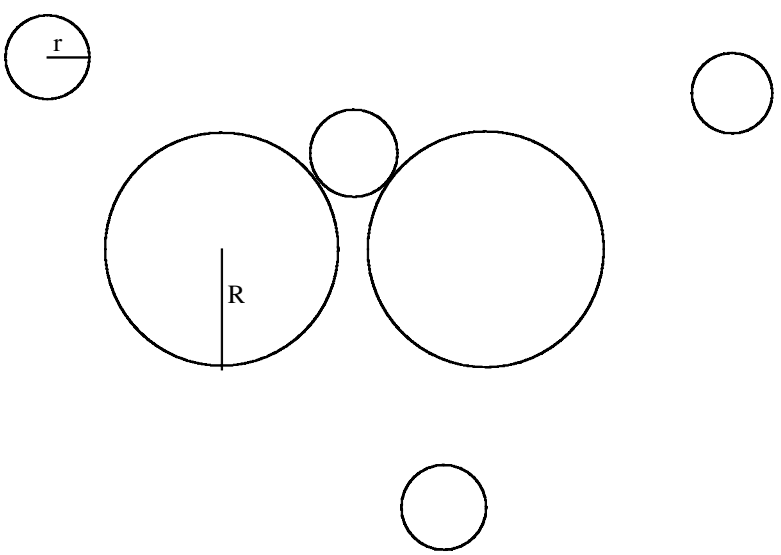

Figure 4. The depletion interaction: two large spheres with surfaces closer than a small-sphere diameter tend to move towards each other to increase the small-sphere entropy.

In the approximation where the small particles are treated as an ideal gas, the attractive well in the effective interaction between the large particles has a depth [49] $\sim k_B T \phi_2 a_1/a_2$, where $k_B T$ is Boltzmann's constant times temperature and ϕ_2 the small-sphere volume fraction. Averaging over the small spheres, the large particles can be thought of as a gas of particles with a short-ranged attractive interaction, and should hence condense [51] when $\phi_2 a_1/a_2$ is of order unity and ϕ_1 is large enough. Whether this 'entropic phase separation' results in a gas–liquid or fluid–solid transition for the large spheres depends [9] on the radius ratio. If $a_1/a_2 \gtrsim 3$ the phase diagram includes gas–liquid coexistence and a critical point, and it is this case which concerns us here.

Studies (e.g. references [52, 53]) of the effects of the depletion force, theoretical and experimental, have focused on *thermal equilibrium* phase behaviour, whereas most practical settings where this force arises involve sedimentation. Here are some examples. In waste-water treatment, small amounts of polymeric additive (the small particles) are used [54] to aggregate and precipitate out suspended impurities (the large particles). Depletion forces arising from small micelles have been used crucially in a fractionation process to produce highly monodisperse oil–water emulsions [55]. In this case the segregated large droplets float up, which is the inverse of sedimentation. The erythrocyte sedimentation rate (ESR) (see, e.g. reference [56]) test used in clinical diagnoses relies on the enhanced rate of settling of red blood cells in the blood of a patient suffering from a serious infection. It is broadly agreed [57] that this enhancement is induced by the increase in the numbers of small proteins in the blood of a very sick patient, although there are debates as to the detailed nature of the mechanism. A depletion-based explanation seems the most likely, especially given the non-specific nature of the enhancement. In addition to the practical issues just mentioned, the large concentration fluctuations near the critical point in the thermal equilibrium phase diagram of bidisperse suspensions presents the possibility of enormous hydrodynamic effects if sedimentation is turned on. The interplay of depletion-induced (or any other) attraction and the hydrodynamics of sedimentation thus presents intriguing new problems in the non-equilibrium statistical mechanics of suspensions.

In section 6 I shall summarize experimental and theoretical work on bidisperse sedimentation. Experiments have been done on Brownian and non-Brownian suspensions. In the former, the emphasis is on the subtle effects of depletion forces on the sedimentation rate [54], whereas in the latter [58] the primary interest is in the types of hydrodynamic instabilities seen in these systems. I shall discuss briefly the problems posed by these studies. Theoretical work on the interplay of sedimentation and phase separation is limited. There are some studies [46] of the effect of a uniform drift field on the critical point behaviour, but all in the absence of the hydrodynamic interaction. I shall concentrate on very recent work on an extension [59] of the Caflisch–Luke [16] and Levine *et al.* [30] approach to include phase separation. Reference [59] observes that phase separation and screening represent opposing tendencies: the former *enhances* concentration fluctuations, and the latter *suppresses* them for small wavenumber normal to gravity. This could lead, for parameter values close to the equilibrium critical point, to microphase separation and ordered columnar structures. No experiments have tested this idea so far.

3. Stokesian hydrodynamics

3.1. *From Navier–Stokes to Stokes*

Recall that the velocity and pressure fields $\mathbf{v}$ and p of a fluid of density ρ and shear viscosity μ obey the Navier–Stokes equation

$$\rho\left(\frac{\partial \mathbf{v}}{\partial t} + \mathbf{v}\cdot\nabla\mathbf{v}\right) = \mu\nabla^2\mathbf{v} - \nabla p + \mathbf{f}, \tag{3}$$

with

$$\nabla\cdot\mathbf{v} = 0 \tag{4}$$

in the incompressible limit. The body force density $\mathbf{f}$ in (3) accounts for gravitational or other forces not subsumed in the pressure. The Reynolds number $\mathrm{Re} = UL\rho/\mu$ is an estimate of the ratio of the inertial ($\rho\mathbf{v}\cdot\nabla\mathbf{v}$) and viscous ($\mu\nabla^2\mathbf{v}$) terms in (3) for a flow with characteristic speed U and length scale L. For the suspensions in which we are interested, taking μ to be the viscosity of water (1 cP), Re ranges from 10^{-6} if L is the particle size to 10^{-4} if we take L to be the interparticle distance. The approximation $\mathrm{Re} = 0$, in which the inertial term $\rho\mathbf{v}\cdot\nabla\mathbf{v}$ is neglected, is thus a very good one for these systems. In addition, on the scale of a typical particle radius of a micron or so, the viscous damping time for the flow of water is $\sim 1\,\mu\mathrm{s}$, so if we are concerned with particle motions on time scales larger than a microsecond, the temporal acceleration term $\partial\mathbf{v}/\partial t$ can also be ignored. In this (singular) limit (3) is thus replaced [9, 60] by the balance of forces known as the Stokes equation:

$$-\mu\nabla^2\mathbf{v} = -\nabla p + \mathbf{f} \tag{5}$$

with $\nabla\cdot\mathbf{v} = 0$. Note that (5) is linear, which means that solutions to it can be superposed, subject to boundary conditions. Let

$$P_{ij}(\mathbf{k}) \equiv \delta_{ij} - \frac{k_i k_j}{k^2} \tag{6}$$

be the projector transverse to the wavevector $\mathbf{k}$ in Fourier space. Then, using incompressibility (4) to eliminate the pressure field from (5) yields

$$-\mu\nabla^2\mathbf{v} = \tilde{\mathbf{f}}, \tag{7}$$

where in Fourier space

$$\tilde{f}_i(\mathbf{k}) = P_{ij}(\mathbf{k})f_j(\mathbf{k}). \tag{8}$$

A remarkable property of the Stokes equation (5) is its *reversibility*. Recall first that the Navier–Stokes equations (3) lack time-reversal invariance (i.e. invariance under inversion of time, velocity and forces), because of the viscous term. The nominal zero-viscosity limit of (3), namely the Euler equations, of course possess this invariance. What is surprising and counterintuitive is that the large-viscosity limit, i.e. the Stokes equation, is also time-reversal invariant, as can be seen by inspection of (5). This has important physical consequences which we will point out briefly in section 3.3. Let us now look at some simple solutions to the Stokes equation.

3.2. *One sedimenting particle*

About a century and a half ago, Stokes [61] solved the problem of a single, non-Brownian, spherical particle of radius a and mass density ρ_p settling steadily and slowly, so that equation (5) applies, in a gravitational field of strength g through an unbounded viscous fluid of mass density $\rho_\mathrm{f} = \rho_\mathrm{p} - \Delta\rho$ and shear viscosity μ. He found that the sphere settled at a speed $v_\mathrm{Stokes} \equiv \frac{2}{9}a^2\Delta\rho g/\mu$. Equivalently, the force

on the particle for a given settling speed v_0 is $6\pi\mu a v_0$. This is of course easy to see qualitatively: the viscous force is the viscous shear stress ($\sim \mu\nabla v \sim \mu v/a$) times the area of the particle ($\sim a^2$). More important, defining the buoyant weight $W = (4\pi/3)\Delta\rho g a^3$, his solution shows that the fluid velocity field

$$\mathbf{v}(\mathbf{r}) = \frac{W}{8\pi\mu a}(\mathrm{I} + \hat{\mathbf{r}}\hat{\mathbf{r}}) \cdot \hat{\mathbf{z}}\frac{a}{r} + \mathrm{O}\left[\left(\frac{a}{r}\right)^3\right] \tag{9}$$

decays very slowly as a function of distance $\mathbf{r}$ from the centre of the sphere. This is to be expected since a single settling particle is a delta-function force in (5).

3.3. *Two sedimenting particles*

Now imagine two particles sedimenting. From (7), each is like a point charge, producing a (velocity) field decaying as the inverse first power of the distance from it, and the velocity due to each advects the other. By naive analogy to electrostatics one might ask whether these 'charges' attract or repel. Two spheres, settling in an unbounded fluid in the Stokesian limit [62], do *neither*: they do not change their relative position. This is an immediate consequence of the invariance, mentioned above, of the Stokes equation under reversal of velocities and forces. If they were to move, say, towards each other when gravity pointed 'down', they would have to move apart when gravity was 'up', whereas these two cases represent the same physical situation, so that the relative motion has to be the same in both cases. In short, since reversing the body force should lead to a reversal of the velocities, the only consistent relative velocity for two identical spheres sedimenting in an unbounded volume is *zero*. This is one of the most striking differences between Stokesian hydrodynamics and the more familiar inertia-dominated case, where Bernoulli's theorem is invoked to explain why fluid flowing between two objects pulls them together.

The joint mobility of a pair of particles as a function of the magnitude and direction of their separation is a crucial input into the theory of sedimenting crystalline suspensions. In figure 3, an external (e.g. buoyancy-corrected gravitational) force $\mathbf{F} = F\hat{\mathbf{z}}$ acts on two spheres of radius a located at $\mathbf{r}_1, \mathbf{r}_2$, with relative and centre-of-mass coordinates $\mathbf{r}$ and $\mathbf{R} = (X, Z)$ (in the plane defined by $\mathbf{F}$ and $\mathbf{r}$, where X and Z are the horizontal and vertical components) respectively, causing them to sediment through a fluid of large shear viscosity μ. The fluid velocity is assumed to obey 'no slip' at the particle surfaces. For our purposes it is enough to work in the dilute limit, i.e. to leading order in a/r. Defining θ to be the angle made by $\mathbf{r}$ with the *horizontal*, with $\theta > 0$ if particle 2 is at a greater height than particle 1, it is straightforward to show starting from (5) [9] that the horizontal and vertical centre-of-mass velocities, in units of the isolated-particle Stokes speed and to leading order in a/r, are

$$\begin{aligned} \frac{\mathrm{d}X}{\mathrm{d}t} &= -\frac{3}{4}\frac{a}{r}\sin\theta\cos\theta, \\ \frac{\mathrm{d}Z}{\mathrm{d}t} &= 1 + \frac{3}{4}\frac{a}{r} + \frac{3}{4}\frac{a}{r}\sin^2\theta. \end{aligned} \tag{10}$$

Physically, this means that the centre-of-mass velocity of a pair of sedimenting particles is different from that of a single sedimenting particle. This difference is larger the closer they are to each other. There are three important aspects to this difference. First, if their separation vector is neither horizontal nor vertical, the

velocity is not directed straight downwards but has a horizontal component as well. This component points towards the horizontal location of the *lower* particle, as if the particle pair is trying to move 'downhill'. Secondly, a tilted pair settles faster vertically as well, in a manner *even* in the tilt. Lastly, both horizontal and vertical drift speeds increase if the particles are brought closer together for a given tilt. These considerations led Crowley [43] to his results on the instability of sedimenting lattices, and are a microscopic justification for the phenomenological equations of motion for drifting crystalline arrays [40, 41]. We shall see this in more detail in section 5.

3.4. *More than two sedimenting particles*

Although it is generally understood that hydrodynamic dispersion [12] (see section 1.1.1) is a result of chaos in the trajectories of the suspended particles, the underlying microphysics was not elucidated until the elegant work of Jánosi *et al.* [13], who showed that the dynamics of three Stokesian particles under a constant external force field was governed by a chaotic saddle. The typical evolution of the three-particle system results in two particles pairing off and moving ahead (since a pair as we noted above moves faster than a single particle), the third being left trailing. The time the three particles spend together before one of them peels off and escapes is found to be highly sensitive to initial conditions, and a positive Lyapounov exponent is found for the dynamics. Presumably the apparently random nature of particle motions in many-particle sedimentation is a result of the processes elucidated in reference [13] for three particles, although I do not know of any attempt to relate the measured hydrodynamic diffusivities to the Lyapounov spectrum.

The above analysis of the three-particle sedimentation problem teaches us that any attempt at an analytical study of the many-particle problem must take into account the chaotic nature of the motion. Whether one studies this N-body problem in terms of particle coordinates [31, 63] or concentration fields [30] is a matter of taste. The point is that it is a problem in *statistical* physics.

4. Velocity fluctuations in steady Stokesian sedimentation: a puzzle and its resolution?

4.1. *Long-ranged effects in sedimentation*

The form of the Stokes equation (5) or (7), in particular the appearance of the Laplacian of the velocity field, is a result of momentum conservation. It is therefore to be expected that a local disturbance would have long-ranged consequences, since the perturbation in the momentum can only be transferred from one region of the fluid to an adjacent region. There are several 'infrared problems' which arise from this long-ranged character of the hydrodynamic interaction. As a simple example, consider a single particle sedimenting along the z direction, and ask how much fluid it drags with it. This is obtained by integrating the z component of the velocity over a plane passing through the particle, with the normal along $\hat{\mathbf{z}}$. Since, as we saw in section 3.2, the velocity $\sim 1/r$ with distance r from the particle, the integral diverges linearly with the size of the system. Clearly the presence of walls is of overwhelming importance: in a real system, this large amount of fluid is recycled by a backflow at the walls.

Batchelor's calculation of the mean settling speed of a dilute suspension presents and solves a related infrared difficulty. Consider a suspension of N particles (heavier than the solvent, hence sedimenting in the $-\hat{\mathbf{z}}$ direction) at positions $\{\mathbf{x}_\alpha\}$. Let $c(\mathbf{r})$ be the number density field at point $\mathbf{r}$, with mean c_0. If the buoyant weight of a particle is W, then the Stokes equation reads

$$-\mu\nabla^2\mathbf{v}(\mathbf{r}) = -\nabla p - \hat{\mathbf{z}}Wc(\mathbf{r}), \tag{11}$$

with $\nabla \cdot \mathbf{v} = 0$. For point particles, this implies that the mean settling speed of a particle at a point $\mathbf{r}_0$ is

$$\mathbf{U}_s(\mathbf{r}_0) = -\hat{\mathbf{z}}U_0 - W\int \mathrm{d}^3r'\mathsf{G}(\mathbf{r}_0 - \mathbf{r}') \cdot \hat{\mathbf{z}}c(\mathbf{r}|\mathbf{r}_0), \tag{12}$$

where $n(\mathbf{r}|\mathbf{r}_0)$ is the number density at $\mathbf{r}$ given that there is a particle at $\mathbf{r}_0$, i.e. it is the pair correlation function between $\mathbf{r}$ and $\mathbf{r}_0$, and the kernel G is the Oseen tensor, whose Fourier transform is

$$G_{ij}(\mathbf{k}) = \frac{P_{ij}(\mathbf{k})}{\mu k^2}. \tag{13}$$

The trouble is that (12) contains an integral which diverges as L^2 for a system of linear dimension L, since $c(\mathbf{r}|\mathbf{r}_0)$ approaches the constant mean number density c_0 for $\mathbf{r} - \mathbf{r}_0 \to \infty$. This is the difficulty that Batchelor [19] resolved, by noting that for any finite container the mean fluid velocity in the suspension is zero: the bottom induces a backflow through the suspension that, on average and in the steady state, cancels the induced velocities. This can be thought of as an order-of-limits problem. In experiments and hence in calculations, one takes a finite system, lets it settle down to a stationary state and and measures its properties, and then studies systems of various sizes in the same manner. Thus, one must take the infinite-time limit first, and then the infinite-size limit. The former limit assures zero mean fluid velocity. This means that the pair correlation function in (12) should be replaced by $c(\mathbf{r}|\mathbf{r}_0) - c_0$. The resulting expression for the settling speed is then finite provided $c(\mathbf{r}|\mathbf{0}) - c_0$ approaches zero faster than r^{-2}. His treatment is equivalent [64] to noting that the mean number density on the right-hand side of reference (11) can be absorbed into a redefinition of the pressure $p_R = p - n_0 Wz$. Physically, this extra pressure gradient is generated by the bottom of the container. Let us now move to the main subject of this section, the divergent variance [16] of velocity fluctuations in hard-sphere sedimentation.

4.2. *The Caflisch–Luke puzzle revisited*

Caflisch and Luke's result [16], and its relation to the small-wavenumber behaviour of concentration fluctuations, can be seen easily from the considerations in section 4.1. Fourier-transforming (11), we see that the fluctuations $\delta\mathbf{v}(\mathbf{k})$ and $\delta c(\mathbf{k})$ in the suspension velocity and concentration at wavevector $\mathbf{k}$ in our suspension of particles with buoyant weight W, sedimenting steadily in the $-z$ direction, are related by

$$\delta v_i(\mathbf{k}) = -W\frac{P_{iz}(\mathbf{k})}{\mu k^2}\delta c(\mathbf{k}) \tag{14}$$

so that the suspension-velocity variance at any point in space, in d dimensions, should be

$$\langle|\delta\mathbf{v}|^2\rangle = \left(\frac{c_0 W}{\mu}\right)^2 \int \frac{\mathrm{d}^d k}{(2\pi)^d} \frac{|P_{iz}(\mathbf{k})|^2}{k^4} S(\mathbf{k}), \tag{15}$$

where the transverse projector P_{ij} was defined in (6), c_0 is the mean concentration, and

$$S(\mathbf{k}) \equiv c_0^{-1} \int \mathrm{d}^d r \langle \delta c(\mathbf{0}) \delta c(\mathbf{r}) \rangle \exp(-\mathrm{i}\mathbf{k}\cdot\mathbf{r}) \tag{16}$$

is the (static) structure factor of the concentration fluctuations. The infrared convergence of the integral in (15) clearly depends crucially on the behaviour of the structure factor at small waveumber. Caflisch and Luke's result, extended to a general space dimension d, and a general structure factor, can be restated thus: if the suspension has no significant *anti*correlations at small wavenumber, so that $S(k \to 0) > 0$, then (15) says that the velocity variance $\langle|\delta\mathbf{v}|^2\rangle$, for $d \leq 4$, diverges at least as strongly as L^{4-d} with the linear dimension L of the container. If on the other hand $S(k \to 0) \to 0$ faster than k^{4-d} (faster than k in 3 dimensions), then $\langle|\delta\mathbf{v}|^2\rangle$ is finite. In more detail, defining

$$\Delta v \equiv \langle|\delta\mathbf{v}|^2\rangle^{1/2}, \tag{17}$$

(15) tells us for $d = 3$ and a structureless $S(k)$ that

$$\frac{\Delta v}{v_{\mathrm{sed}}} \sim \left(\phi \frac{L}{a}\right)^{1/2}, \tag{18}$$

where $\phi \sim c_0 a^3$ is the volume fraction, a the particle radius and L the linear dimension of the container. CL do not tell us the form of $S(k)$: as with the renormalized settling-speed calculation of Batchelor, the CL result too *assumes* a particle distribution and looks at its consequence for the velocity. This is true for Hinch's version [18] of the derivation of the CL result as well. Note that for a collection of N particles

$$S(k \to 0) = \frac{\langle N^2\rangle - \langle N\rangle^2}{\langle N\rangle} \equiv \frac{\sigma_N^2}{\langle N\rangle}, \tag{19}$$

where $\langle . \rangle$ denotes an average over the fluctuations. If the number fluctuations were perfectly random, as in an ideal gas, one would expect the number variance $\sigma_N^2 = N$, i.e. $S(k \to 0) = 1$; if they had a weak tendency to cluster (anticluster) then $\sigma_N^2 \propto N$ with a constant of proportionality greater than (less than) unity. A vanishing $S(k \to 0)$ implies that the number fluctuations are *qualitatively* smaller than those resulting from purely random variation, i.e. that $\sigma_N^2 = \langle N^2\rangle - \langle N\rangle^2$ grows more slowly than constant$\times N$ for large N.

We shall return to these points shortly when we discuss recent theoretical developments. Let us first survey the experiments in some detail.

4.3. *Experiments on velocity fluctuations in steady sedimentation*

As summarized in section 2.1.2, a wide range of techniques has been used to probe the spatiotemporal structure of velocity and concentration correlations in sedimentation. I summarize their findings here.

4.3.1. *Tagged-sphere measurements*

Koglin [23] and Tory *et al*. [20] marked, radioactively or otherwise, a few submillimetre-sized spheres in a sedimenting suspension at volume fractions ranging from 10^{-3} to 10^{-2} and measured traversal times for a fixed vertical distance, typically of the order of a metre, or the vertical distance covered in a fixed time of the order of a minute. From the scatter in these measurements they inferred the variance in the sphere velocities. On the assumption that the CL [16] divergence should be cut off by finite-size effects on a scale equal to the distance to the nearest boundary, they argue that the velocity variance should peak when the particle is halfway between the free surface and the bottom. The scatter in the data for settling times is indeed consistent with this rough picture. However, their findings cannot rule out a finite screening length of order, say, half the vertical height of the fluid column in the container. More important, all their measurements are for the *initial* variance; this means that the suspension quite possibly retains a memory of the initial randomly stirred state, which presumably has no correlations or anticorrelations in the particle positions. The anticorrelations which could be present in the structure factor of the true steady state in, say, the fluidized bed geometry, would be artificially suppressed and, consequently, the velocity variance would diverge with system size.

Ham and Homsy [24] and Nicolai and Guazzelli [25] followed large (hundreds of μm diameter) glass beads, silvered but hydrodynamically identical to the index-matched particles forming the bulk of the suspension, again in batch settling, in a standard organic fluid about a thousand times as viscous as water, and measured their hydrodynamic diffusivities. In reference [25] these are studied directly as functions of system size ranging (smallest dimension) from 2 to 8 cm, whereas in reference [24] the approach is similar to that of reference [20] in that the dependence on settling distance is monitored. In reference [25] the probability distribution of the velocities and the velocity autocorrelation function were measured. A very significant anisotropy in the diffusivities is noted, but neither reference [25] nor reference [24] finds any size dependence.

4.3.2. *Swirls from particle imaging velocimetry*

The experiments of Segrè *et al*. [17] measure the suspension velocity field, coarse-grained on the scale of a couple of particle sizes, by particle imaging velocimetry [65] on a suspension of monodisperse, effectively hard-sphere particles of polystyrene, of radius of about 8 μm. The sealed glass sample cells used were rectangular parallelepipeds with dimensions from $3\,\text{mm} \times 0.3\,\text{mm} \times 50\,\text{mm}$ to $30\,\text{mm} \times 10\,\text{mm} \times 200\,\text{mm}$, and a cylinder of height 30 mm and radius 0.5 mm. In all the cells, the line of sight was in the direction which was rather narrower than the rest. Volume fractions from 0.01 to 5% were studied. The illuminated area was about $0.4 \times 0.5\,\text{mm}^2$, the plane of focus was the midplane of the cell, and the depth of focus was about 0.5 mm. These studies were not done in the fluidized bed state, but in batch sedimentation, where a dispersion of particles was shaken vigorously and allowed to settle partly. Measurements were taken well away from both the settling front at the top of the suspension and the sedimenting layer at the bottom, on the assumption that this middle region, statistically speaking, was relatively homogeneous and stationary. Their main finding is that the velocity standard deviation ΔV, scaled by the mean V_{sed} grows with the width W of the sample for a range of W but then saturates for L greater than a *correlation length* $\xi \propto a\phi^{-1/3}$, where a is the particle radius and ϕ is the particle volume fraction. A plot of

$\Delta V/V_{\text{sed}}\phi^{1/3}$ versus $W/a\phi^{-1/3}$ yields an impressive data collapse, reinforcing the significance of the mean interparticle spacing $a\phi^{-1/3}$ as a characteristic length scale for sedimenting suspensions. They also estimate ξ from the spatial correlation function of the velocity field, and find consistent results. An important qualitative observation of this work is that the velocity fluctuations are in the form of swirls whose size is of the order of ξ. The only difficulty with this work, as Brenner [21] points out, is that it studies the dependence on the *width*, which is not the smallest dimension of the cell. There *is* some data for the dependence on the depth, which is indeed the smallest dimension, and it *is* consistent with screening on a scale ξ, but there is not enough of it for a firm conclusion. It is not known, moreover, whether the velocity-fluctuation data collapse is independent of the thickness (the smallest dimension of the cell), a question raised in Brenner's critique [21] (see section 4.5.2). None the less, it is the most detailed study to date of the spatial correlations of sedimenting velocity fields.

4.3.3. *Sound-scattering studies*

In the experiments of Cowan *et al.*, a fluidized bed of 0.4 mm glass beads in a glycerol–water mixture was studied in a cell with length × width × thickness = 20 cm × 12 cm × 0.776 or 1.22 cm [26]. The Peclet number was about 10^{11}. The probe used for these studies was *sound* scattering spectroscopy. In this technique, analogous to dynamic light scattering (for single scattering) [66] or diffusing wave spectroscopy [67] when the probe beam is highly multiply scattered, a plane wave pulse is incident on the sample and the near-field speckle of the scattered beam is autocorrelated. The theory for interpreting these measurements is, as in references [66] or [67], dependent on the scattering regime. The measurements give information about the time evolution of the displacements of the scatterers, here the suspended particles. The importance of this work lies in the Reynolds number (Re) range studied. Re was varied from 0.007 to 0.3 by changing the fraction of glycerol. This appreciable variation in Re was found to have no perceptible effect on the nature of velocity correlations. The velocity variance was found to be finite as in reference [17], with a screening length that showed no dependence on the smallest dimension of the cell. This work thus suggests (a) there *is* an intrinsic screening mechanism at work and (b) that inertia has no role to play in it, ruling out one suggested mechanism for screening [21], since varying the viscosity by a factor of 400 changed nothing.

4.3.4. *Light-sheet measurements of number fluctuations*

Lei *et al.* [22]† have recently carried out the only direct test to date of particle number fluctuations in sedimentation. Working at Peclet number $> 10^6$ and Reynolds number $\sim 10^{-7}$, they studied the evolution of the number fluctuations starting from an initially highly stirred and hence structureless suspension. They used polystyrene spheres about 40 μm in diameter, at volume fractions of about 0.004, in a rectangular cell measuring $1 \times 1 \times 4\,\text{cm}^3$ (so that their measurements were not affected by the proximity of walls) and imaged the positions of the particles by means of a 0.35 mm thick light-sheet slicing vertically through the sample. A patch of the slice, measuring a few mm^2, was imaged through a microscope/CCD attachment.

† This approach was first taken by Smith [68], but the test volume in that work was insufficient [35].

They found that the statistics of number fluctuations went from Poissonian at early times when, presumably, the particles are distributed randomly because of the initial stirring, to strikingly sub-Poissonian at later times as the long-range hydrodynamic effects of sedimentation set in. In other words (see section 4.2) σ_N^2/N *decreases* with N for large N, which means $S(k \to 0) \to 0$. Quantitative comparisons of these measurements with theories [30, 31, 35] of the small-wavenumber structure factor in sedimentation are as yet unavailable. The qualitative trend in favour of a strong suppression of number fluctuations (i.e. of an anticorrelation of concentration fluctuations at large length scales, and hence of a possible escape from the Caflisch–Luke divergence) is however clear, although I am concerned that the estimated screening lengths are larger than the beam thickness.

4.3.5. *Velocity fluctuations: a summary*

In brief, then, experiments on the velocity-fluctuations problem have not reached a consensus. There is evidence for and against the Caflisch–Luke scenario of a divergent velocity variance. Part of the difficulty lies in the fact that rather different geometries have been used in the various experiments, leaving open the possibility that nearby walls could suppress long-range hydrodynamic effects. Almost all of the measurements are in the batch-settling mode rather than in the fluidized-bed geometry; the sample is initially shaken, and measurements are taken after some time (say, after the sedimentation front has settled some modest fraction of the cell height, but before settling is complete, or some such rule of thumb). There is thus some question whether true steady-state properties are being measured. From the point of view of testing theories of sedimentation, it is highly desirable that experiments work in geometries where stationarity is assured and side walls do not obscure the true long-range effects of the hydrodynamic interaction. Further experiments are thus required to settle unambiguously the question of the nature of steady-state sedimentation. Theoretical studies of the problem, meanwhile, will inevitably focus primarily on trying to understanding the phase diagram of steadily sedimenting particles in unbounded containers. We turn next to a summary of numerical simulation studies of steady sedimentation, followed by a survey of theoretical approaches to the problem.

4.4. *Simulations of sedimentation*

Brenner's [21] simulations represent the particles sedimenting while confined between two infinite walls as point forces suitably augmented by images. The velocity field due to each point force is cut off at small length scales as a way of putting in an effective particle size and avoiding unphysical singularities. Since this simulation was used mainly to test theoretical ideas about the effect of walls, I shall not spend much time on it here; a summary of Brenner's analytical work is in section 4.5.2. The simulations of Ladd [27] are the most extensive numerical search for screening or its absence. Fluid flow in Ladd's simulations is implemented using a lattice Boltzmann approach: an occupation probability is assigned to directed bonds from each site of a three-dimensional cubic lattice to nearest and next-nearest neighbours. The surfaces of the suspended particles are internal 'boundary nodes' at which, in effect, no-slip boundary conditions are imposed, and the particles are moved by the fluid flow. This approach is known [69] to reproduce the equations of suspension hydrodynamics. Ladd studies up to 32 768 particles, i.e. 32 particles on a side in a cubic box, with periodic boundary conditions, and measures velocity variances and particle pair

distribution functions. Over the range of sizes studied, the velocity variance grows linearly with the smallest dimension of the system, and the structure factor for the particle concentration does not appear to go to zero at small wavenumbers. For box sizes up to 70 particle radii and volume fractions from 0.01 to 0.1, there is no screening. The dependence of relaxation times τ on length scale W, moreover, is $\tau \sim W^{1/2}$, in agreement with reference [70] and behaviour predicted for the *unscreened phase* in reference [30] (see section 4.5.4 below).

It is none the less important that the large-distance behaviour of the pair distribution function shows distinct deviations from that expected for a purely random suspension. If we define the pair correlation function

$$g(\mathbf{r}) \equiv N^{-1} \sum_{i \neq j} \langle \delta(\mathbf{r} - \mathbf{R}_{ij}) \rangle, \tag{20}$$

where $\mathbf{R}_{ij}$ is the separation vector between the ith and jth particles in a collection of N particles at volume V, then it is straightforward to show that the condition $S(\mathbf{k} \to 0) = 0$ on the structure factor, as the wavenumber k goes to zero, is equivalent to the requirement that

$$n(r) \equiv \frac{N}{V} \int \mathrm{d}^3 r' [g(\mathbf{r}') - 1] \tag{21}$$

approach -1 as r grows; this has to be done for various finite and increasing N and V, keeping r small compared to $V^{1/3}$. Ladd [27] finds $n(r)$ to be distinctly smaller than that for a truly smaller suspension, although well above -1. Thus, in Ladd's simulations, there appears to be some tendency to suppress small-wavenumber concentration fluctuations, but not enough to produce screening.

It is of course conceivable that there is a screening length much larger than 70 particle radii (10 to 20 interparticle spacings at these volume fractions), or that there is a screened phase outside the range of volume fractions explored.

We turn next to analytical, theoretical approaches to the velocity-variance problem. These include proposals for how screening could come about, as well as one study [21] which takes the Caflisch–Luke argument for granted but analyses its consequences when the no-slip boundary condition at nearby walls is included.

4.5. *Theories of the velocity variance in steady sedimentation*

4.5.1. *Confined fluid flow*

We noted above that many experiments, e.g. those of reference [17], are performed in containers with one dimension (the y dimension, i.e. the thickness, normal to the xz plane of view) much smaller than the other two. This is a serious shortcoming, as pointed out by Brenner [21], who remarks that Segre *et al*. [17] find growth and saturation of the velocity variance as a function of the *largest* rather than the smallest dimension of the container. Before presenting his arguments, we digress briefly to study the nature of fluid flow in a confined quasi-two-dimensional geometry [71, 72]. Purely as a result of the incompressibility constraint, this flow still has a long-ranged aspect although the hydrodynamic interaction is screened by the walls. This can be seen as follows. The fluid velocity field $\mathbf{v}$ satisfies the Stokes equation (7) in the interior of the container; if the thickness is D, then no-slip boundary conditions at the walls mean that the longest allowed wavelength in the y direction is $\sim D$. Thus, the Stokes equation in the presence of a body force $\mathbf{f}(\mathbf{r})$ can

be averaged over the y direction to give an effective equation relating the effective (y-averaged) two-dimensional velocity and force fields $\mathbf{U}$ and $\mathbf{F}$:

$$(\gamma - \mu\nabla_{xz}^2)\mathbf{U} = \tilde{\mathbf{F}}, \tag{22}$$

where $\gamma \sim \mu D^{-2}$ is a Darcy-like friction coefficient resulting from the confinement between the walls and, in two-dimensional Fourier space with coordinates $\mathbf{K}$,

$$\tilde{F}_i(\mathbf{K}) = P_{ij}(\mathbf{K})F_j(\mathbf{K}), \tag{23}$$

is the two-dimensional transverse projection of $\mathbf{F}$. At large length scales in the xz plane, the gradients on the right-hand side of (22) can be ignored relative to γ; equations (22) and (23) then imply a $1/r^2$ decay with distance r in the xz plane from a localized force density, simply as a result of transverse projection, and not because of any long-ranged hydrodynamic interaction, the latter having been killed by the walls. The $1/r^2$ has, naively speaking, the same dimension as a two-dimensional delta-function, but is in fact long-ranged—although not enough to make a serious difference, as we shall now see. Repeating the arguments of section 2.1.1 for this case implies that the velocity variance due to a collection of random localized concentration fluctuations now comes from summing r^{-4} over a two-dimensional array of points labelled by r. The dominant contribution to this comes from small r, and is thus determined by the short-distance cut-off ($\sim$ the particle size). The large r contribution goes as $r^2/r^4 \sim r^{-2}$ and hence converges.

4.5.2. *Brenner's critique*

Brenner [21] argues that the hydrodynamic effects of a particle's force density are screened once the particle reaches the wall. For a container with thickness $\ll$ the other dimensions, this effect could be very significant. If a particle starts from the centre of the container, it has a vertical velocity v_{sed} and a transverse fluctuation velocity Δu. Its lateral wandering as it settles will take it to the nearest wall, a distance D (the thickness) away in a time $\tau \sim D/\Delta u$, by which time it will have fallen a distance $\ell = \text{constant} \times v_{\text{sed}}D/\Delta u = \text{constant} \times D(a/\ell\phi)^{1/2}$, where the second equality is based on (18) evaluated on a length scale ℓ. This self-consistently determines

$$\ell \sim a^{1/3}D^{2/3}\phi^{-1/3} \tag{24}$$

and

$$\frac{\Delta u}{v_{\text{sed}}} \sim \left(\frac{D}{a}\right)^{1/3}\phi^{1/3}, \tag{25}$$

as in reference [17]. Note that (24) and (25) show a cube-root dependence on the particle size a and an explicit dependence on the smallest dimension D; this can be used as a crucial test of Brenner's ideas. Preliminary indications from experiments† are in favour of a *linear* dependence on a, contrary to (24). Brenner's simulations, however, appear to be consistent with his theoretical arguments. One statement by Brenner is misleading: early in the paper, he says that the observation of extended spatial correlations in reference [17] contradicts the assumption of pair interactions. It should be clear that local, pairwise interactions are perfectly capable of leading to

† Segrè *et al.*, in unpublished work referred to in reference [35], have verified that the screening length $\xi \sim a\phi^{-1/3}$ for a from 3 to 7.8 μm.

long-ranged correlations or anticorrelations: neither screening nor the absence of it is evidence against two-body interactions, contrary to Brenner's assertion.

That, then, was Brenner's conservative explanation of the observations of reference [17]: no true screening, just the effect of walls, but in a form more subtle than a naive application of the Caflisch–Luke result to a confined system would yield. It could well be the correct explanation of the Segrè *et al.* screening, but it is unclear how it accounts for the Ham–Homsy [24] and Nicolai–Guazzelli [25] observations, which are performed in containers which are quite wide in all directions. The size dependence, moreover, is monitored in reference [25] by varying the *smallest* dimension of the cell, and in reference [24] by looking at the diffusivity as a function of how far a particle has settled. One possible worry about these experiments as well, as noted by Brenner, is that since they sample particles at all locations in the cell, and the hydrodynamic diffusvities are smaller near the walls, the samples would be biased in favour of particles near the walls. If this bias yielded a disproportionate number of particles within a fixed distance of the wall, independent of container size, the result could be an apparently size-independent variance. The only sure test, therefore, is one which samples particles exclusively in the bulk. The work of Lei *et al.* [22] mentioned above is a likely candidate. In any event, it should not be long before unambiguous experimental evidence for or against screening are available.

4.5.3. *Koch and Shaqfeh's screening theory*

The first theoretical approach to the possibility of screening in steady sedimentation came from Koch and Shaqfeh (KS) [31]. They argued that a structure factor $S(k)$ that vanished sufficiently fast as the wavenumber $k \to 0$ would render the velocity variance finite. They noted further that this required the introduction of a length scale R_s such that $S(k) \ll 1$ for $kR_s \ll 1$, so that the Caflisch–Luke result (18) for the velocity variance would then be replaced by

$$\frac{\Delta u}{v_{\text{sed}}} \sim \left(\phi \frac{R_s}{a}\right)^{1/2}. \tag{26}$$

Before explaining how such a screening length could arise as an intrinsic consequence of the hydrodynamics of the suspension, they drew an important analogy with electrolytes: number-density fluctuations in sedimentation are very much like charge-density fluctuations in electrolytes. A local number-density fluctuation in a sedimenting suspension gives rise to a long-range velocity field, just as the charge density in an electrolyte produces a long-ranged electrostatic potential. The suspension velocity field moves the particles just as the electric field moves the charges. The long-ranged electrostatic interaction in an electrolyte solution results in a charge-density structure factor that vanishes at zero wavenumber [73]. Might one not expect the number-density structure factor likewise to vanish at zero wavenumber in a sedimenting suspension?

Inspired by this analogy KS [31] carried out a calculation of pair correlations in steady sedimentation, as follows. Consider a sedimenting suspension with mean concentration n, and let $n^3 m(\mathbf{x}, \mathbf{r})$ be the joint probability of finding a pair of particles with separation $\mathbf{r}$ with magnitude of order the particle size a, i.e. a 'close pair', and a third particle at relative position $\mathbf{x}$ with $x \gg a$. Note that by definition $m(\mathbf{x}, r \to \infty) = 1$ since the probability density for finding three well separated and

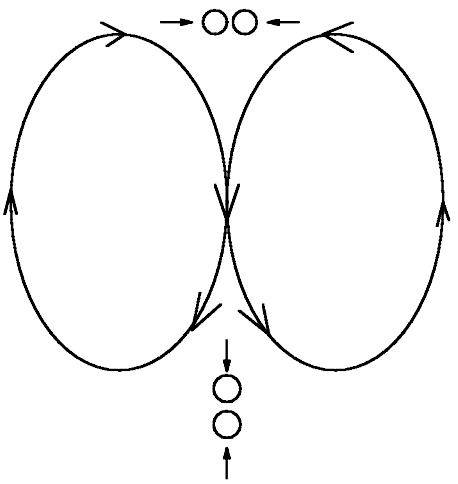

Figure 5. Koch and Shaqfeh's pictorial explanation for a particle deficit around a sedimenting particle: the extensional part of the flow produced by the particle promotes horizontal pairs above and vertical pairs below.

hence independent particles is simply n^3. Let $n^2\Omega(\mathbf{r})$ be the probability of finding two particles with separation $\mathbf{r}$ with $r = O(a)$. Then the probability of finding the third particle at x so large that the close pair is unaffected by it is clearly $n^3\Omega(\mathbf{r})$. KS then calculate the pair distribution function and velocity correlations for a sedimenting suspension using $\Omega(\mathbf{r})$ as input. This they do by calculating the behaviour of triplets of particles, focusing on the effect of the remote third particle on the flow around the close pair. They argue that the extensional component of this induced flow is such as to favour horizontally separated close pairs at locations above the third particle and vertically separated close pairs below it. The former pairs settle [9] more slowly than the latter. This gives rise to a nett deficit of pairs near any given 'third' particle, assuming the close pair probability, which is the input to the calculation, is uniform, i.e. $\Omega(\mathbf{r}) = 1$. This turns out, in their calculation, to yield the necessary long-range particle deficit (see equation (21)) and consequently a finite variance for the velocity. It is not clear, however, that the simple pictorial explanation they offer (figure 5) is really at work; their mechanism is a fluctuation effect.

In more detail, their calculation expresses the N-particle probability in terms of contributions from m and Ω as defined above, and neglects 4-body and higher correlations. A conservation law for $m(\mathbf{x}, \mathbf{r})$ is constructed, taking into account movements of the three particles, along with Stokesian hydrodynamic expressions for the relative velocity of the the close pair and the distant third particle. The resulting expression for the structure factor shows screening. The consequent finite variance σ_v^2 of the velocity is calculated and found to be about 4 times the square of the Stokes speed U_s. An approximate expression for the particle diffusivity D in terms of the Fourier-transformed spatial correlation function of the velocity field is obtained, and shown to yield $D \sim U_s a\phi^{-1}$, where a and ϕ are respectively the particle radius and volume fraction. Equivalently, the screening length is shown to go as $a\phi^{-1}$ which does not, however, agree with the experiments of reference [17].

There are some features of the KS calculation which are hard to reconcile with more standard approaches to statistical Stokesian hydrodynamics. For example,

their general expression for the relation between the structure factor $S(\mathbf{k})$ and the velocity variance σ_v^2 (notation of this review, not KS's paper) can be written as

$$\sigma_v^2 = \frac{c_0}{\mu^2}\int \frac{\mathrm{d}^3k}{(2\pi)^4}\frac{|P_{iz}(\mathbf{k})|^2}{k^4}[2 - S(\mathbf{k})]S(\mathbf{k})S(-\mathbf{k}). \tag{27}$$

Equation (27), as Ladd [75] remarks, is rather different in detail from the straightforward relation (15). This difference is probably a consequence of the way in which KS develop their expansion for the induced velocity in terms of *conditional* probabilities. The validity of this expansion seems somewhat uncertain, and this difference may be responsible for some of the disagreement between their theory and those of references [30] and [35].

None the less, the KS theory thus shows how—within a certain approximate calculational scheme—to relate the bare or short length-scale correlation function $\Omega(\mathbf{r})$ of a sedimenting suspension to the observed macroscopic structure factor. It is not a completely predictive theory, in that it cannot in addition calculate $\Omega(\mathbf{r})$ for a suspension of a given volume fraction at $\mathrm{Pe} = \infty$, $\mathrm{Re} = 0$. This is not a drawback in itself. The problem is that it only shows that a particular form of Ω leads to screening. This is hard to test in simulations or experiments: what is needed is a categorization of all suspensions into those that screen and those that do not, based on some easily calculated property of Ω. This could then be turned into a predictive if phenomenological phase diagram of steady sedimentation. The approach of Levine *et al.* [30] achieves this, in a continuum stochastic PDE framework.

4.5.4. *Fluctuating hydrodynamics of steady sedimentation*

Levine *et al.* [30] argue that it is sufficient to treat the forces in the Stokes equation at a monopole level, but that the concentration should obey a stochastic advection–diffusion equation. The effects of higher multipoles are irrelevant in the mean but are argued to result, along with close encounters of three or more particles, in a noise source as well as hydrodynamic diffusivities in the equation for the concentration. I present below the arguments leading to their equations of motion. The description is phenomenological, but only to the same extent as a continuum Ginzburg–Landau model or its time-dependent analogue for an equilibrium phase transition problem such as phase separation in a binary fluid.

The following general principles are crucial to the construction of these equations of motion. (i) Since the aim is to write down a description valid at asymptotically large length and time scales, only the most slowly-varying fields need to be included. Away from a critical point, these would in general be [33] (a) the 'conserved modes', i.e. the local densities of independently conserved quantities and (b) 'broken-symmetry' variables corresponding to motions which at zero wavenumber become continuous symmetry transformations. (ii) Since the suspension has not undergone a phase transition into a state where a continuous invariance (e.g. translation, rotation) is spontaneously broken, there are no broken-symmetry modes. This leaves only the conserved modes which, for an incompressible suspension, are the local concentration of suspended particles and the total (solute + solvent) momentum density. (iii) As already noted in section 1, the microscopic Stokesian dynamics of a sedimenting suspension is spatiotemporally chaotic. Anything short of a *complete* specification of initial conditions will lead, therefore, to indeterminacy in the

dynamics. In such a situation, one cannot in general hope to obtain analytical expressions for the statistical properties of the system starting from the exact microscopic dynamical equations. The coarse-grained effective description for the long-wavelength degrees of freedom will contain *stochastic* terms (a direct effect of the eliminated fast degrees of freedom) as well as diffusive terms (an indirect effect), both involving phenomenological parameters. This step is no more controversial than starting with an isolated system of many interacting particles governed by the laws of non-dissipative, Hamiltonian classical mechanics, and replacing the fast degrees of freedom by noise [76] to obtain the generalized Langevin equations that are the standard description of time-dependent fluctuations at thermal equilibrium. The only difference is that the noise in sedimentation is not constrained by requirements such as a fluctuation–dissipation theorem, because sedimenting systems are *driven*, held in a state far from thermal equilibrium. The general idea that driven non-Brownian suspensions are stochastic is enunciated by Leighton and Acrivos [77] and particularly emphatically by Tory *et al.* [20]; the latter even propose stochastic equations of motion, but different in spirit from and less general than those proposed here. Indeed, any treatment of the statistical properties of suspensions can be recast in terms of noise-driven equations of motion. The noise, as will shortly be seen, is simply a convenient calculation tool. Since only a limited range of modes (say, with wavenumbers larger than a cut-off scale Λ, of order an inverse interparticle spacing) have been eliminated, the resulting noise can have correlations only on scales smaller than $\Lambda^{-1} \equiv \ell$. The noise in the effective equations can be thought of as containing velocity fluctuations beyond the point-force approximation and hydrodynamic reflections involving groups of particles with separation less than the coarse-graining scale ℓ. The resulting noise source must perforce consist of random particle currents with no correlations over space and time scales larger than ℓ and a corresponding time τ_ℓ. As far as a description on scales $\gg \ell$ and a corresponding time scale τ_ℓ is concerned, the noise can be treated as spatially and temporally uncorrelated. The magnitudes of the noise variance and the corresponding hydrodynamic diffusivities [12] at the scale ℓ in a strictly non-Brownian system must, on dimensional grounds, be of order $v_{\rm sed}\ell$, where $v_{\rm sed}$ is the Stokesian settling speed. In laboratory experiments, there will in principle be additional Brownian contributions to noise and diffusion. While knowledge of the detailed properties of the noise would require a direct numerical solution of the problem†, its general features, such as the form of its covariance, should once again be governed by the symmetry principles enunciated above. (iv) To get the long wavelength physics right, it is useful to work at leading order in a gradient expansion. (v) At this leading order in gradients, it is essential to keep all terms *not explicitly forbidden* on grounds of symmetry, and impose *no* relations amongst the phenomenological parameters other than those *mandated* by the symmetries of the problem. In particular, as remarked above, no fluctuation–dissipation relation can be assumed to hold in general between the noise and diffusivities. Note that the model makes only an innocuous assumption about the short-time, local effects of an elimination of the fast variables. The large-scale, long-time behaviour is *calculated* from the coarse-grained equations of motion given below. This approach lends itself easily to the many well-controlled analytical

† See, for example, Hayot *et al.* [78], where the 2-dimensional Kuramoto–Sivashinsky equation, which is deterministic but linearly unstable, is shown to be equivalent to a stochastic PDE with a positive diffusivity.

techniques developed in the study of continuum models of critical dynamics and allied phenomena [79, 80].

Once accepted these premises lead inevitably, for a suspension sedimenting steadily along the $-z$ direction, to a stochastic advection–diffusion equation

$$\frac{\partial \delta c}{\partial t} + \delta \mathbf{v} \cdot \nabla \delta c = (D_{0\perp} \nabla_\perp^2 + D_{0z} \nabla_z^2) \delta c + \nabla \cdot \mathbf{f}(\mathbf{r}, t) \tag{28}$$

for the concentration fluctuation δc at space point $\mathbf{r}$ at time t, and the Stokes equation (see equation (7))

$$\mu \nabla^2 \delta v_i(\mathbf{r}, t) = m_R g P_{iz} \delta c(\mathbf{r}, t) \tag{29}$$

for the suspension velocity fluctuation δv, with incompressibility imposed by means of the transverse projector P_{ij}. Equation (28) contains the advection of the concentration by the velocity and, as argued at the beginning of this subsection, an anisotropic 'bare' hydrodynamic diffusivity $(D_{0\perp}, D_{0z})$ and a spatiotemporally white noise or random particle current $\mathbf{f}(\mathbf{r}, t)$. The latter is taken, reasonably, to have Gaussian statistics with mean zero and covariance

$$\langle f_i(\mathbf{r}, t) f_j(\mathbf{r}', t') \rangle = c_0 (N_{0\perp} \delta_{ij}^{\perp} + N_{0z} \delta_{ij}^{z}) \delta(\mathbf{r} - \mathbf{r}') \delta(t - t'), \tag{30}$$

where c_0 is the mean concentration, and δ_{ij}^{z} and $\delta_{ij}^{\perp}$ are respectively the projectors along and normal to the z axis. In a perfectly non-Brownian system with settling speed v_{sed}, particle size a one expects $N_{0\perp}$, N_{0z}, $D_{0\perp}$, $D_{0z} \sim v_{sed} a$, as argued earlier in this section. However, no further relation between the noise and the diffusivities may be assumed, since this is a non-equilibrium system. In particular, and this is crucial, the 'fluctuation–dissipation ratio'

$$R_{fd} \equiv \frac{N_{0\perp} D_{0z}}{D_{0\perp} N_{0z}} \tag{31}$$

may not in general be set to unity. Since at equilibrium the ratio of noise strength to kinetic coefficient is a temperature, the departure of R_{fd} from unity measures the anisotropy of the non-equilibrium analogue of a 'temperature' for this driven system. The idea of a temperature for non-Brownian sedimentation is to be found in reference [29] as well.

It is easy to see that deviations if any from the CL result of a divergent variance must come from the advective nonlinearity $\mathbf{v} \cdot \nabla c$: if we ignore this nonlinearity, then the structure factor (16) can be computed by straightforward Fourier transformation of (28), giving

$$S(\mathbf{k}) = S_0(\mathbf{k}) \equiv \frac{N_{0\perp} k_\perp^2 + N_{0z} k_z^2}{D_{0\perp} k_\perp^2 + D_{0z} k_z^2}. \tag{32}$$

The form of (32) depends on the direction k of the wavevector, but not on its magnitude. This means that (32), in the absence of the advective nonlinearity, does not mitigate the CL [16] divergence (see equation (15)). The form of (32) does imply real-space correlations decaying in d dimensions as $1/r^d$ with distance r, if $R_{fd} \neq 1$, as has been discussed in the general context of driven diffusive systems [81]. We shall discuss below the implications of this for the complete nonlinear theory.

Using (29) to eliminate the velocity field in (28) turns the latter into a stochastic diffusion equation for the concentration alone, with a quadratic nonlinearity (cubic

vertex, from the point of view of diagrammatic perturbation theory, and hence a three-body coupling, in particle language):

$$\frac{\partial \delta c}{\partial t} + \lambda \nabla \cdot \left[\delta c(\mathbf{r}) \int_{r'} \mathsf{G}(\mathbf{r}_0 - \mathbf{r}') \cdot \hat{\mathbf{z}} \delta c(\mathbf{r}') \right] = (D_\perp \nabla_\perp^2 + D_z \nabla_z^2) \delta c + \nabla \cdot \mathbf{f}(\mathbf{r}, t). \quad (33)$$

The nonlinearity in (33) couples concentration fluctuations widely separated in space. This important feature is clearly related to the types of three-body coupling discussed by KS [31] (see section 4.5.3), and was shown [30] to lead to screening under certain conditions. To see how to include the effects of this nonlinear vertex, note first that the expression (32) for the structure factor in the linearized theory is of the form

$$\frac{\text{Noise strength}}{\text{Relaxation rate}}. \quad (34)$$

When the nonlinear coupling in (33) is included, the structure factor can still be written in the form (32) or (34), provided the 'bare' quantities (with subscript '0' in (32)) are replaced by suitably renormalized noise strengths $N_\perp(\mathbf{k}), N_z(\mathbf{k})$ and a renormalized relaxation rate $R(\mathbf{k})$:

$$S(\mathbf{k}) = \frac{N_\perp(\mathbf{k}) k_\perp^2 + N_z(\mathbf{k}) k_z^2}{R(\mathbf{k})}, \quad (35)$$

where the form of the relaxation rate has deliberately not been written merely in terms of renormalized diffusivities, for a reason which will become clear shortly.

Before we see how to carry out this renormalization, a comparison with the dynamics of screening in electrolytes (the statics of which is discussed in detail in reference [73]) is useful. For simplicity we treat the charges as moving in a passive frictional medium, so that solvent hydrodynamics is ignored. Let ρ be the relative concentration of + and − charges in the electrolyte (analogous to high and low concentration fluctuations in a sedimenting suspension). Suppose first that the + and − were just labels rather than charges. Then there is only an interdiffusion current and a corresponding noise:

$$\frac{\partial \rho}{\partial t} - D \nabla^2 \rho = \nabla \cdot \mathbf{f}, \quad (36)$$

where the relative diffusivity D and the spatiotemporally white noise $\mathbf{f}$, with covariance N, obey a fluctuation–dissipation relation. The static structure factor for the 'charge' density is then N/D, a non-zero constant at zero wavenumber. When the Coulomb interaction and Ohm's law are included, of course, (36) is modified to

$$\frac{\partial \rho}{\partial t} - D \nabla^2 \rho - \nabla \cdot \mathbf{j}_E + \nabla \cdot \mathbf{f}, \quad (37)$$

where the conductivity σ gives an Ohmic current $\mathbf{j}_E = \sigma \mathbf{E}$ due to the electric field $\mathbf{E} \equiv -\nabla \Phi$, and the electric potential Φ obeys

$$\nabla^2 \Phi = -\rho. \quad (38)$$

Equations (37) and (38) are the analogues of (28) and (29), with an important difference: the effect of the electric field enters linearly in the electrolyte problem, while in (28), as a result of incompressibility, the velocity enters only at *bilinear* order. It is easy to see that (37) and (38) imply a structure factor

$$S_\rho(k) = \frac{Nk^2}{\Gamma_\rho(k)}, \tag{39}$$

where the 'renormalized' relaxation rate

$$\Gamma_\rho(k) = \sigma + Dk^2 \tag{40}$$

for charge density fluctuations at wavenumber k. Thus, charge-density fluctuations on length scales larger than

$$\xi_\rho \equiv \left(\frac{D}{\sigma}\right)^{1/2} \tag{41}$$

are suppressed strongly, and relax anomalously rapidly, at an essentially wavenumber-independent rate $\Gamma_\rho(0)$ [82]. One way of looking at this is that the Coulomb interaction induces a non-local relaxation of the charge density, while the noise remains local and conserving. The general expression (34) then tells us that the structure factor must vanish at zero wavenumber.

Returning to the sedimentation problem, we then see that if the hydrodynamic interaction gives rise to wavenumber-independent relaxation of the number density, while leaving the noise unchanged, screening should result. This cannot happen as simply to concentration fluctuations in sedimenting suspensions because, as stated above, the long-range advection of the concentration by the velocity (the analogue of the Ohmic current in the electrolyte problem) enters only at nonlinear order (see equation (33)). The question therefore is whether the advective nonlinearity leads in (35) to a renormalized relaxation rate $R(\mathbf{k} \to \mathbf{0}) \neq 0$. This is answered [30] by calculating $N_\perp(\mathbf{k})$, $N_z(\mathbf{k})$ and $R(\mathbf{k})$ in a diagrammatic perturbation expansion (see, e.g. [80]). The expression (35) connects noise, diffusion and structure factor. It is thus clear that one could describe the perturbation theory in terms of a renormalized structure factor and relaxation rate, never mentioning the noise explicitly. This in effect is what approaches like those of reference [31] do. In that sense the introduction of a noise term is not a radical step, but merely a calculational device for generating the perturbation expansion.

Galilean invariance [30] protects the advective vertex from graphical corrections at leading order in wavenumber. We need therefore only calculate the self-energies for the noise and the relaxation rate, i.e. the difference between the renormalized quantities in (35) and their bare values in (32). These can be expressed [30] in terms of integrals over products of dynamic correlation functions and propagators of the concentration field, which themselves contain the self-energies, and must therefore be evaluated self-consistently.

Consider first some general properties of the correction $\Delta R(\mathbf{k}) \equiv R(\mathbf{k}) - (D_{0\perp}k_\perp^2 + D_{0z}k_z^2)$, evaluated at lowest order in (non-self-consistent) perturbation theory. Although this object is formally infrared divergent in three dimensions, its structure is important as the starting point for self-consistent or renormalization group calculations. It turns out [30] to have two qualitatively distinct pieces:

$$\Delta R(\mathbf{k}) = \Delta_1(\mathbf{k})k^2 + \gamma(\mathbf{k})\frac{k_\perp^2}{k^2}. \tag{42}$$

In (42), Δ_1 renormalizes the diffusivities, while the key quantity is the term involving γ, which is (a) not of a type present in the bare equation (32) or (28), (b) non-zero only if $k_\perp \neq 0$, (c) not diffusive and (d) proportional to $\mathrm{sgn}\,(R_{\mathrm{fd}} - 1)$ where the

fluctuation–dissipation ratio R_{fd} was defined in (31). We can rationalize the above proportionality of Δ_1 to sgn $(R_{fd} - 1)$ (setting $D_z = D_\perp$ for simplicity) by looking at the effect of a noise-injected concentration fluctuation (NICF) on an imposed macroscopic concentration inhomogeneity. If $N_z \gg N_\perp$ the typical NICF varies predominantly along z and the induced z velocity alternates in sign mainly along z thus reinforcing the inhomogeneity. However, if $N_\perp \gg N_z$, the NICF and hence the sign of the resulting z velocity both vary mainly in the xy plane, so that the flow breaks up the inhomogeneity and thus enhances effective diffusion. In any case, the γ term is absent if the bare noise and bare diffusivities obey a fluctuation–dissipation relation ($R_{fd} = 1$). In reference [30], they ignore the intriguing case $R_{fd} < 1$ where a *negative* relaxation rate (i.e. a possible instability) could arise, and construct a phase diagram for the regime $R_{fd} > 1$. Conveniently, the renormalization of the *noise* has a structure like that of Δ_1, with no γ-like term. Screening can thus arise if a self-consistent calculation gives $\gamma(\mathbf{k} \to \mathbf{0}) > 0$.

4.5.4.1. *Self-consistent screening.* A complete calculation including the renormalizations of all the coefficients in (33) is not yet available. However, [30] seeks a solution of the form (42) with $\gamma(k \to 0) \equiv \gamma_0 > 0$. This leads to a 'self-consistent' equation for γ_0 which has a solution only if the anisotropy parameter $K \equiv R_{fd} - 1$ is larger than a calculable critical value K_c. For γ_0 large, $\Delta_1(k \to 0)$ and the corresponding noise correction are non-singular and indeed negligibly small, so that the diffusivities and noise strengths can be set to their bare values. As $K \downarrow K_c$, the self-consistent answer for γ_0 goes continuously to zero. In this manner, Levine *et al.* [30] predict two phases (figure 6) for steady sedimentation, screened ($\gamma_0 > 0$) and unscreened ($\gamma_0 = 0$), separated by a continuous non-equilibrium phase transition at which $\gamma_0 \to 0$ and hence the screening length

$$\xi_{sed} \equiv \sqrt{\frac{D_{0\perp}}{\gamma_0}} \tag{43}$$

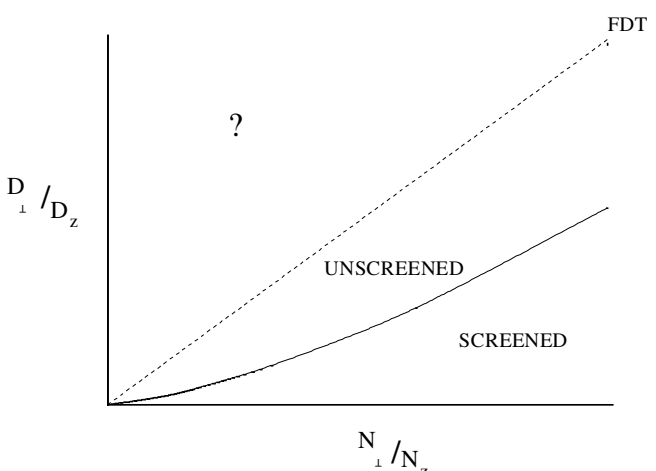

Figure 6. Levine *et al.*'s non-equilibrium phase diagram for steady sedimentation: FDT denotes the line on which a fluctuation–dissipation theorem is obtained, and the question mark is a region where the calculation breaks down because of singular negative fluctuation corrections to the relaxation rate.

diverges as $(K - K_c)^{-1/3}$ in their self-consistent approximation, and scales as $a\phi^{-1/3}$ deep in the screened phase, in agreement with reference [17].

Levine *et al.* [30] make detailed predictions for the behaviour of concentration and velocity correlation functions in the screened phase (which appear to be consistent with the preliminary observations of reference [22]; see section 4.3.4). More important, although it is unclear how the phenomenological parameters of their theory are related to microphysics, an independent test of the theory can nonethe-less be made by measuring the bare (i.e. large wavenumber) noise and diffusivity parameters, and seeing if the values locate the system in the screened or the unscreened region of the phase diagram (figure 6). The bare diffusivities can be obtained from self-diffusion measurements, while the ratios of noise to diffusion coefficients are contained in the structure factor.

4.5.4.2. *The unscreened phase.* For $0 \leq K < K_c$, this simple approach in which the diffusivities and noise strengths are not renormalized is insuffucient, since $\gamma_0 \to 0$ as $K \downarrow K_c$. A more complete calculation has still not been carried out. However, for $K = 0$, i.e. $R_{fd} = 1$, where a fluctuation–dissipation (FD) relation holds, and hence a $\gamma(\mathbf{k})$ (see equation (42)) is never generated, the steady state is known exactly [30]. This leads to a constant, direction-independent zero-wavenumber structure factor, hence a divergent Caflisch–Luke velocity variance $\sigma_v^2 \sim L$, and a highly superdiffusive relaxation rate $R(k) \sim k^{1/2}$. This behaviour, which is also predicted by [70] and seen in the simulations of reference [27], is expected to hold throughout the region $0 < K < K_c$, not only at the FD line $K = 0$. Note that the unscreened phase has no analogue in electrolytes.

It is clear from reference [30] and indeed from reference [31] (see section 4.5.3) that screening and its absence are both possibilities in a general phase diagram for steady sedimentation. It is reasonable to ask how an experimenter could move around in such a phase diagram. In the absence of a microscopic theory, the most one can say is that at zero Reynolds number the parameter K can depend only on Peclet number Pe and particle shape [70]. Decreasing Pe (i.e. increasing the role of *thermal* Brownian diffusion) by reducing the mass-density difference between particles and solvent is likely to make the effective temperature more isotropic, driving the system into the unscreened phase. Working with particles of various forms (prolate, oblate, perhaps polymer coated so that another length scale is introduced) is another possibility, but it is unclear just where in the phase diagram would lead.

One drawback of the approach of reference [30] should be noted. The screening length ξ was predicted to scale as $a\phi^{-1/3}$, which is just the interparticle distance. This phenomenological theory is unable to make a quantitative prediction for the coefficient. Unless ξ is a large number times $a\phi^{-1/3}$, the continuum hydrodynamic description is questionable on scales small compared to ξ. It is therefore reassuring that Segrè *et al.* [17] find $\xi \simeq 17a\phi^{-1/3}$, although until the criticisms of Brenner (see section 4.5.2) of those experiments are answered this cannot be taken as definitive.

4.5.5. *An analogy to high Prandtl number turbulence*

Tong and Ackerson [35] note that the advection–diffusion (28) and Stokes (29) equations are identical to those for the Rayleigh–Bénard convection problem in the Boussinesq approximation [83] if the concentration field in the sedimentation problem is identified with the temperature field in convection. Denoting characteristic velocity and length scales by U (say the mean settling speed) and L (the

container size, ignoring anisotropy), defining the kinematic viscosity ν, and recalling that non-Brownian suspensions with particle size $a \ll L$ have a purely hydrodynamic diffusivity $D_h \sim Ua$, we see that for Reynolds number $\mathrm{Re} \equiv UL/\nu \to 0$, the suspensions have $\nu/D_h \sim \mathrm{Re}^{-1}L/a \to \infty$. In the convection problem this translates to an infinite ratio of ν to the thermal diffusivity, i.e. Prandtl number $\mathrm{Pr} \to \infty$. The analogy to turbulence is not forced: the sedimenting suspension too is in a driven, spatiotemporally chaotic state, but this is high Peclet (rather than Reynolds) number turbulence. The authors speculate about the origin of the concentration fluctuations that give rise to these random velocity fluctuations, suggesting that Crowley's [43] (see section 5.1) is involved. The latter is however the instability not of a uniform concentration field but of a spatially periodic state; the work of Jánosi *et al.* [13] is more likely to provide the explanation.

Scaling lengths by L and time by L^2/D_h, and working in terms of $\delta\psi$, the volume fraction fluctuation scaled by its mean ϕ_0, the Stokes equation (29) when non-dimensionalized becomes $\nabla^2 \delta u_i = \mathrm{Ra}\delta\psi P_{iz}$, where

$$\mathrm{Ra} \equiv \frac{m_R g}{\mu D_h}\left(\frac{L}{a}\right)^3 \phi_0 \sim \left(\frac{L}{a}\right)^3 \phi_0 \tag{44}$$

(since $D_h \sim Ua$ and $U \sim m_R g/\mu a$) is the analogue here of the Rayleigh number in the convection problem, and the limit of interest is clearly $\mathrm{Ra} \to \infty$. Tong and Ackerson interpret in the context of sedimentation the arguments of Kraichnan [84] and Priestley [85] for a characteristic length scale in high-Prandtl-number turbulence as follows. I have recast their reasoning in an easily applicable form: the typical velocity fluctuation $\delta u(\mathcal{L})$, generated by concentration fluctuations, scales (via Caflisch–Luke) as $U(\phi_0\mathcal{L}/a)^{1/2}$. This velocity fluctuation has an associated Péclet number $\mathrm{Pe}(\mathcal{L}) = \delta u(\mathcal{L})\mathcal{L}/D_h$. It follows that at a scale $\mathcal{L} = \delta_d \sim \mathrm{Pe}_c^{2/3} a \phi_0^{-1/3}$, $\mathrm{Pe}(\mathcal{L})$ attains the value Pe_c for the transition to Péclet-driven turbulence with $\mathrm{Re} \ll 1$. At length scales above δ_d, the flow must enter a different regime where large-scale advection prevents concentration variations. The velocity variance is thus cut off, yielding $\delta u/U \sim \mathrm{Pe}_c^{1/3}\phi_0^{1/3}$, consistent with references [17] and [30]. The numerical estimates of coefficients in reference [35] are also in quite good agreement with reference [17]. This scenario is not an alternative to references [30, 31], but a qualitative description of the detailed screened-phase behaviour of reference [30]. In particular, although reference [35] does not state this explicitly, the suppression of concentration fluctuations by large-scale advection (i.e. a vanishing small-wavenumber structure factor) is implicit in the ideas of reference [84]. The drawbacks of this approach are that it ignores the anisotropic nature of sedimentation and that it is a set of persuasive arguments rather than a detailed calculation. Its success at predicting not only the scaling properties but their amplitudes as well is none the less impressive.

This concludes our discussion of the velocity fluctuations problem. Much remains to be done here. Experiments must address themselves to the truly stationary state of a fluidized bed, in a geometry where the walls are far from the region of interest; a complete fluctuating hydrodynamic theory, preferably in a dynamical renormalization-group framework, is clearly essential, as is a connection between the phenomenological parameters in reference [30] and microscopic quantities such as particle shape, Brownian Péclet number and volume fraction. I believe this important problem in the statistical mechanics of driven systems can then be settled in the near future.

5. Clumping instabilities and anomalous coarsening in crystalline fluidized beds

We noted in section 2.2 that crystalline suspensions are usually made out of particles heavier than the suspending fluid, and are thus generally in a state of sedimentation. Such a suspension in, say, a fluidized bed geometry is thus one realization of an important non-equilibrium steady state, namely an ordered but deformable lattice drifting through a dissipative medium. We remarked that such a state also arises in the case of a flux-point lattice drifting through a slab of clean type II superconductor. Although this latter problem has been studied intensively [39], especially with a view to understanding the effects of quenched disorder, the analogous problem for suspensions has received very little attention. This section will summarize the theoretical papers [40–43] that specifically address the question of the stability of steadily sedimenting crystalline suspensions. The important literature on the settling speed of rigid crystalline arrays [19] will not be surveyed, but experiments [37] which offer evidence for the effect of fluctuations on the settling speed, and could be extended to study the instability proposed in references [40, 41, 43] will be discussed. We shall assume that we are working far from the equilibrium phase transition from the crystalline to a fluid-like suspension [6]. The interplay of sedimentation and freezing [86, 87] will not be discussed.

5.1. *Crowley's experiments and theory*

Crowley [43] considered arrays of hard spheres with radius a, settling in a viscous fluid in the Stokesian approximation. In the simplest model he considered, which is sufficient for our purposes, the hydrodynamic interaction was truncated at the nearest neighbour level. He considered perturbations $(\xi_n(t), \eta_n(t))$ in the positions of the particles (labelled by the index n) as a function of time t in a one-dimensional array with spacing $d \gg a$ parallel to the (horizontal) x axis and drifting (under gravity, for example) with a mean speed U in the vertical z direction. Scaling lengths by d and times by d/U, his equations for the perturbations read:

$$\left.\begin{aligned} \frac{\partial \xi_n}{\partial t} &= +\frac{3}{4}\frac{a}{d}(\eta_{n+1} - \eta_{n-1}), \\ \frac{\partial \eta_n}{\partial t} &= -\frac{3}{4}\frac{a}{d}(\xi_{n+1} - \xi_{n-1}). \end{aligned}\right\} \tag{45}$$

These equations can be obtained from (10) in section 3.3. It is easy to see that (45) implies that a sinusoidal perturbation with small (non-dimensional) wavenumber K will *grow* at a rate $\beta = (3/2)(a/d)K$.

Ordered arrays settling steadily in a viscous fluid are thus unstable to clumping and buckling at small wavenumbers (figure 7). Crowley's experiments on 1/16 inch steel balls settling in Venice turpentine (viscosity $\sim 10^4$ P) confirmed this instability. However, the arrays in Crowley's work are not true crystalline suspensions, but are simply particles prepared in an initially ordered configuration. His analysis thus does not include elastic restoring forces, Brownian motion (or the analogous random motions induced by hydrodynamic dispersion) and nonlinearities, all of which could in principle resist this instability in a suspension of micron-sized polymer spheres in a charge-stabilized crystalline state. The work of references [40, 41], to which we turn next, takes these forces into account.

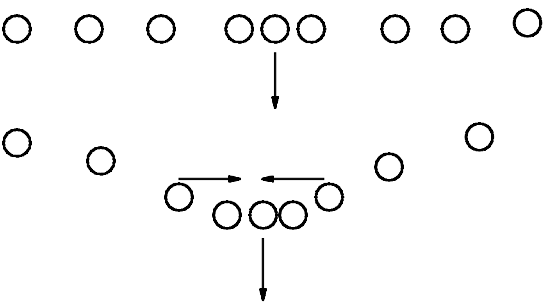

Figure 7. Crowley's mechanism: pairs settle faster than isolated particles, and tilted pairs settle obliquely, leading to a clumping and buckling instability.

5.2. *The long-wavelength dynamics of drifting crystals*

As we have seen in sections 4 and 3, local variations in the concentration of a sedimenting suspension are carried to arbitrarily large length scales by the long-ranged hydrodynamic interaction. A complete analysis of the sedimentation dynamics of a three-dimensional crystalline suspension thus requires the explicit inclusion of the hydrodynamic velocity field, as in the preceding section. Crowley's analysis got around this by truncating the hydrodynamic interaction. This simplification can be applied to a physically realizable situation [28], namely a crystalline suspension with lattice spacing d, sedimenting in the $-z$ direction, in a container with dimensions $L_x \sim L_z \gg L_y \sim d$ (figure 8).

The *local* hydrodynamics that leads to the Crowley instability [40, 43] is left unaffected by this, but the long-ranged hydrodynamic interaction is screened in the xz plane on scales $\gg L_y$ by the no-slip boundary condition at the walls, as we discussed in section 4.5.1. The model equations (47) in dimension $d = 2$ apply to such a system. Hydrodynamic effects should be important locally in such a set-up if d is somewhat larger than a.

As a result of the confined geometry, the system reduces to a two-dimensional crystal lying in the x–z plane and drifting along $\hat{\mathbf{z}}$. References [40, 41] treat this

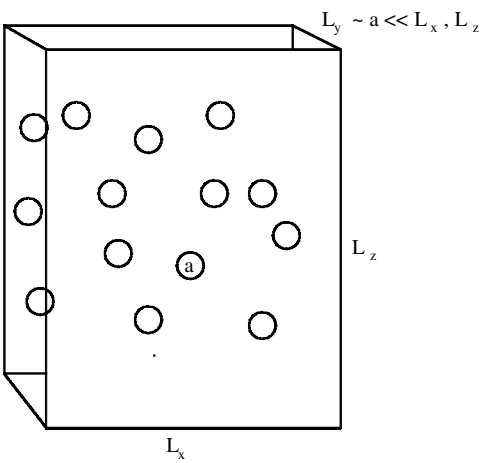

Figure 8. A suspension confined between walls to screen out long-ranged hydrodynamic effects, giving a quasi two-dimensional system.

system on scales large compared to d as a continuum and describe local distortions of the drifting crystal by means of the Eulerian displacement field $\mathbf{u} = (u_x, u_z)$. We shall see shortly how Crowley's instability enters the dynamics. Note first that the equations of motion for $\mathbf{u}$, ignoring inertia, as is appropriate for the suspensions of interest, are of the form VELOCITY = MOBILITY × FORCE, i.e.

$$\frac{\partial}{\partial t}\mathbf{u} = \mathsf{M}(\nabla\mathbf{u})(\mathsf{K}\nabla\nabla\mathbf{u} + \mathbf{F} + \mathbf{f}). \tag{46}$$

In reference (46), the first term in parentheses on the right-hand side represents elastic forces, governed by the elastic tensor K, the second ($\mathbf{F}$) is the applied force (gravity, in this case) and $\mathbf{f}$ is a noise source of thermal and/or hydrodynamic origin. In the absence of the driving force $\mathbf{F}$ the linearized dynamics of the displacement field in this inertialess system is purely *diffusive*: $\partial_t u \sim \nabla^2 u$, with the scale of the diffusivities set by the product of a mobility and an elastic constant. Note that we have taken the local mobility tensor M to depend on gradients of $\mathbf{u}$, since such a dependence is not ruled out by any symmetry. The new physics in these equations when the driving force is non-zero, in particular Crowley's instability, will be seen to arise precisely through this strain dependence of M. For a two-dimensional crystal drifting along $\hat{\mathbf{z}}$ in the x–z plane, with $x \to -x$ symmetry, expanding M in powers of $\nabla\mathbf{u}$, (46) becomes

$$\dot{u}_x = c_1\partial_z u_x + c_2\partial_x u_z + \mathcal{O}(\nabla\nabla u) + \mathcal{O}(\nabla u\nabla u) + f_x, \tag{47a}$$

$$\dot{u}_z = c_3\partial_x u_x + c_4\partial_z u_z + \mathcal{O}(\nabla\nabla u) + \mathcal{O}(\nabla u\nabla u) + f_z. \tag{47b}$$

Ignoring nonlinearities and diffusion-like terms for now, (47) says that a tilt ($\partial_z u_x$ or $c_2\partial_x u_z$) produces a lateral drift, and that local changes in the concentration ($\partial_x u_x$ or $\partial_z u_z$) change the settling speed. The coefficients c_i, $i = 1$ to 4 and those that would appear in front of the $\mathcal{O}(\nabla u\nabla u)$ have units of velocity; their magnitude is set by the mean drift speed times the sensitivity of the mobility to local distortions. These are truly non-equilibrium terms, which vanish when the driving force is turned off. If the $\mathcal{O}(\nabla\nabla u)$, $\mathcal{O}(\nabla u\nabla u)$ and noise (f_x and f_z) terms are ignored, and all variation along the z direction neglected, (47) becomes the continuum limit of Crowley's equation (45), making the correspondence $(\xi_n, \eta_n) \to (u_x, u_z)$, with $c_2 = -c_3 = 3aU/2d$. Equations (47) are thus the natural generalization of Crowley's ideas to include elasticity, nonlinearity and noise, and the instability he found obliges us to study them in the *linearly unstable* case $c_2c_3 < 0$. An obvious and important consequence of their form is that the effects of elasticity, at least within a linear theory, are *subdominant* at small wavenumber to the $\{c_i\}$ terms arising from sedimentation. Thus, ignoring nonlinearities, Crowley's instability, with a growth rate linear in the wavenumber k, cannot be suppressed by effects associated with the elasticity of the lattice, which enter at order k^2. Thus, in this linearized treatment, a steadily settling lattice is always unstable to clumping and buckling at small enough wavenumber, no matter how low the settling speed. Nonlinearities and noise together with the stabilizing large-wavenumber effects of elasticity could conceivably shift the instability to a non-zero speed (like a T_c renormalization in critical phenomena [74]), but it is exceedingly difficult to take these into account in the framework of equations (47): symmetry allows ten independent terms bilinear in $\nabla\mathbf{u}$ and six linear second derivative terms, with as many independent coefficients. Lahiri *et al.* [40, 41] introduced a useful simplification, namely, a one-dimensional model (spatial

variations only with respect to x) but retaining *two* dynamical fields u_x and u_z. Further, they note that the local dynamics of the sedimenting crystal depends crucially on (a) whether the concentration is larger or smaller than the mean and (b) whether the local tilt ($\partial_x u_z$) is, say, uphill or downhill to the right. Since (47) is linearly unstable, the concentration perturbation $\partial_x u_x$ and the tilt $\partial_x u_z$ will grow exponentially and without bound in a linearized treatment. Physically, since real colloidal crystals are made of impenetrable particles, and since the elasticity of the lattice will not tolerate arbitrarily large shear strains, the description implicit in (47) of small distortions about a perfect lattice must break down in conditions of unstable growth. It is best, therefore, to work from the outset with naturally bounded variables for the concentration and tilt. To this end, references [40, 41] use a description in terms of the concentration fluctuation field

$$\sigma(x,t) = \frac{\partial u_x}{\partial x} \tag{48}$$

and the tilt field

$$\tau(x,t) = \frac{\partial u_z}{\partial x}, \tag{49}$$

and replace the stochastic PDEs for $\sigma(x,t)$ and $\tau(x,t)$ implied by the one-dimensional reduction of (47) by a discrete stochastic dynamical model with two distinct Ising variables, the concentration fluctuation σ_i with states + and − and the tilt variable τ_i with states denoted / and \ on the odd and even sublattices of a one-dimensional lattice. These evolve with 'spin-exchange' dynamics simply because the corresponding continuum variables, being x derivatives of displacements, are trivially 'conserved modes'. This description was used in reference [41] to show that the simplified model defined by reducing (47) to one dimension is unstable to clumping and buckling, at any non-zero noise strength, if $c_2 = -c_3$. Since such phase separation takes place in this *one*-dimensional model, it is reasonable to expect that it would happen *a fortiori* in a more realistic two- or three-dimensional model. This suggests that real crystalline fluidized beds are always unstable, a prediction that should be testable in experiment. We shall return to this question later in this section. Let us first see how the result was obtained for the one-dimensional model.

The essential physics described just below equation (47) is encoded in the update rules for the evolution of $\{\sigma_i\}$ and $\{\tau_i\}$. The probabilities $W(.)$ per unit time for the various possible exchanges can be represented succinctly [40, 41] by

$$\left.\begin{aligned}
W(+\backslash - \to -\backslash +) &= D + a \\
W(-\backslash + \to +\backslash -) &= D - a \\
W(-/+ \to +/-) &= D' + a' \\
W(+/- \to -/+) &= D' - a' \\
W(/+\backslash \to \backslash +/) &= E + b \\
W(\backslash +/ \to /+\backslash) &= E - b \\
W(\backslash -/ \to /-\backslash) &= E' + b' \\
W(/-\backslash \to \backslash -/) &= E' - b'
\end{aligned}\right\} \tag{50}$$

where the first line, for example, represents the rate of $+-$ going to $-+$ in the presence of a downtilt \, and so on. The quantities D, E, D', E' (all positive) and a, b, a', b' are all in principle independent parameters. A little reflection will show that the case of physical interest and relevance to the sedimentation problem is $\operatorname{sgn} a = \operatorname{sgn} a'$, $\operatorname{sgn} b = \operatorname{sgn} b'$; for simplicity, and without losing any of the essential physics we take $E = E'$, $b = b'$. The linear instability condition $c_2 c_3 < 0$ in equation (47) implies $ab > 0$. The long-wavelength dynamics implied by these rates can be argued [40, 41] to be identical to that of the stochastic PDEs (47) reduced to a one-dimensional form.

It is noteworthy that this change of description has established a link between the sedimentation problem and the widely studied problem of driven diffusive lattice gases [46, 88–91]†‡§. In addition, the one-dimensional coupled nonlinear PDEs of [40] have been shown to be related to models of magnetohydrodynamics [92], drifting polymers [93] and passive scalars on fluctuating surfaces [94].

Working with periodic boundary conditions, and denoting a configuration of the $\{\sigma_i\}$, $\{\tau_i\}$ by C, the dynamics (50) can be shown [41], when $\sum_i \sigma_i = \sum_i \tau_i = 0$ (i.e. there are equal numbers of pluses and minuses, and the mean macroscopic slope is zero) to obey detailed balance with respect to the steady-state distribution

$$\mu_{\mathrm{SS}}(C) = \exp\left[-\beta \mathcal{H}(C)\right], \tag{51}$$

with

$$\mathcal{H} = \epsilon \sum_{k=1}^{N} h_k\{\tau\}\sigma_k \tag{52}$$

provided

$$\frac{b}{E} = \frac{a}{D}. \tag{53}$$

The 'Hamiltonian' (52) can be interpreted as the energy of particles (the σs) moving in a hill-and-valley landscape provided by the $\{\tau_i\}$, if we define the 'height' at site i by

$$h_i\{\tau\} = \sum_{j=1}^{i} \tau_j. \tag{54}$$

With this interpretation the update rules (50) say (figure 9): a peak tends to sink and become a valley if there is a $+$ atop it; a $-$ at the bottom of a valley tends to lift it and make it a local peak; a $+$ tends to move downhill and a $-$ uphill. It is clear that this will eventually lead to macroscopic phase separation, a state in which there is one single valley and hence, with periodic boundary conditions, a single peak, separated by half the system size. From the bottom of the valley until halfway up is occupied by 'pluses', the remainder by 'minuses' (figure 10). A typical rate-limiting step through which the stochastic motion of $\{\sigma_i, \tau_i\}$ in a finite system of size N could dissolve this macroscopically phase-separated state [40] is for a $+$ to climb up to the top of a hill, which would take a time of order $\exp N/4$. This qualifies as true phase separation.

---

† The lattice models of [40] are reviewed briefly by Ramaswamy *et al.* [89].

‡ Barma and Ramaswamy [90] compare and contrast the model of reference [40] with other physically plausible coupled lattice gas models.

§ Evans [91] reviews phase transitions in one-dimensional non-equilibrium systems like those of reference [40].

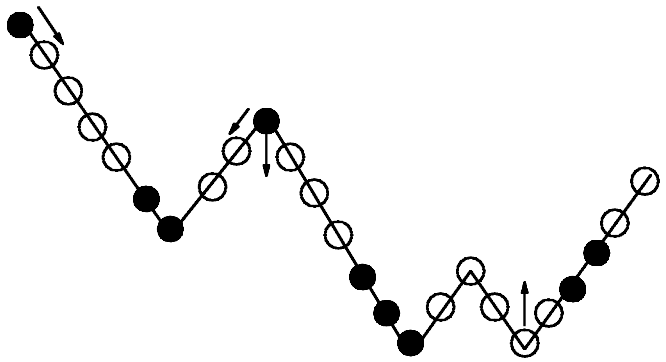

Figure 9. The dynamics of the driven lattice gas for sedimenting crystalline suspensions: filled circle = +; open circle −; + moves downhill, − moves uphill; + makes peaks sink, − makes valleys rise.

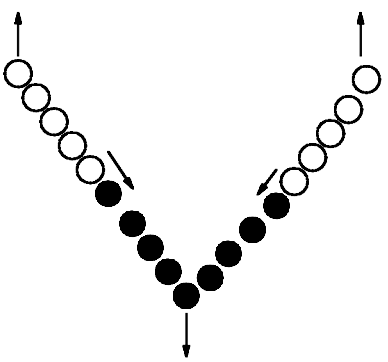

Figure 10 The final state of the model of Lahiri and Ramaswamy for sedimenting lattices is macroscopically phase separated. Oblique arrows show the direction in which the pluses move; vertical arrows denote the evolution of the height profile.

The form (52), (54) of the hidden effective Hamiltonian governing the steady-state distribution of this non-equilibrium model explains why the system manages to phase separate in one dimension: $\mathcal{H}$ is *non-local* if expressed in terms of σ_i, τ_i, local but locally unbounded if written in terms of the height variable (54), so that the usual rules [95] preventing phase separation in one space dimension do not apply. I should add that although these results have been presented in the special limit where detailed balance holds, the behaviour predicted can be shown [41] to hold for the whole range $ab > 0$ in (50) corresponding to the linearly unstable case $c_2 c_3 < 0$ of (47). Moreover, in the infinite system limit, no process succeeds in opposing this tendency: the system is phase separated at any finite (i.e. less than infinite) noise strength. In reference [41] this unusually robust segregation, first reported in reference [40], is called strong phase separation and has also been seen in related models [91, 96].

Remarkably, despite this inexorable tendency to phase separate, the *kinetics* of coarsening is anomalously slow. Consider a system that had phase separated into *four* macroscopic domains, each of size $N/4$. For this state to achieve complete phase separation, i.e. to become two domains of size $N/2$, the two + domains, each at the

bottom of a valley, must merge. The rate-limiting step can again be taken to be the movement of a + from the edge of an all −+ region to the top of a hill, i.e. a distance $N/8$. This will of course take a time of order $\exp(N/8)$, by the same argument as in the previous paragraph, which implies that the characteristic domain size grows logarithmically in time [41, 89], a remarkable result for a system without quenched disorder.

5.3. *Experiments on crystalline fluidized beds*

The experiments reported in references [37, 38] are the only ones I am aware of that study the steady-state settling of crystalline suspensions. Although they remark on the possibility of an instability, they focus on testing predictions [19] of the settling speed of rigid crystalline aggregates as a function of volume fraction. They find in general that the settling is faster than predicted, and that the deviation is greater, the softer the crystal. This points to a role of fluctuations in the lattice structure in determining the settling speed.

Let us turn now to how the predictions discussed in this section could be tested in experiments. Since strong phase separation has been predicted [40, 41] in a *one-dimensional* caricature, it should certainly be seen in real two-dimensional steadily sedimenting crystalline suspensions in, for example, the confined fluidized bed geometry [28] described at the beginning of section 5.2. A good candidate system is a charge-stabilized crystalline array of polystyrene spheres with radius in the micron range. The lattice spacing of the crystal should be neither so large that hydrodynamic effects (proportional to the ratio of particle size to interparticle spacing) are negligible, nor so small as to choke the flow. Note that the model equations (47) were formulated to describe the nature of distortions about a single crystalline domain. In particular, the instability towards clumping takes place only on large enough length scales where the linear first derivative terms dominate the diffusive terms coming from the elasticity. In a polycrystalline sample, if the size of the crystallites is too small, terms from the elastic energy in (47) could dominate instead, on scales within each domain. In addition, it is important that the sedimentation be steady, a requirement best met by working in the fluidized-bed geometry. Observations in reference [38] suggest that strongly charge-stabilized crystalline suspensions appear stable whereas suspensions in a fluid state display the Crowley instability in a visible manner. It is very likely that the instability is present even in the crystalline suspensions, but is masked either by finite crystallite size or by the logarithmically slow coarsening of domains. A search for this last feature, using particle imaging or ultrasmall-angle light scattering, although it might tax the experimenter's patience, would be the most stringent test of the theory presented in this section.

6. The statistical physics of bidisperse sedimentation

6.1. *Sedimentation and the depletion force*

Most suspensions in the real world are mixtures of many types and sizes of particles. Blood is a prime example, and its sedimentation is of great importance in a clinical test called the erythrocyte sedimentation rate (ESR) [56]. The ESR is generally found to be enhanced in the presence of serious conditions such as septicaemia [97]. The reason for this increase is the enhanced aggregation of the red blood cells (RBCs) into 'rouleaux' (columns) which then settle more rapidly (see

section 3.3 and [9]) than individual RBCs. It is now reasonably clear [57] that the microscopic mechanism for this aggregation is the depletion force [49, 51], also known as macromolecular crowding [98]. This well-known phenomenon in colloid science, which I have discussed already in section 2.3, is most simply described for mixtures of large and small spheres, say, of radii R and r respectively because when the surfaces of two large spheres are less than a distance r apart, the small spheres cannot enter the region between the large ones. This loss of entropy can be relieved by having the large spheres move even closer together. This entropy-induced attraction has by now been studied in many experiments on model colloids (see, e.g., references [52, 53]).

In industrial applications, coarse particles, several tens of microns in size, suspended in water are frequently removed by sedimentation. This separation process is known to be enhanced by the addition of much finer particles with size in the 10–100 nm range, which promote the aggregation of the coarser particles. The systematics of this process have been studied by Chu *et al.* [54] who show that when there are appreciable short-ranged spatial correlations between the small particles, the effective interaction between the large particles has a great deal more structure than the simple attractive well with depth $\sim k_B T(R/r)\phi_{\text{small}}$ obtained when the small particles are treated as an ideal gas [49]. The dependence of sedimentation rate on the volume fraction of added small particles is also shown consequently to be non-monotone. The theoretical treatment of reference [54] is, however, also carried out for a system at thermal equilibrium, and sedimentation simply superposed as a property simply determined by the sizes of the aggregates. The long-ranged hydrodynamic interaction is ignored as well. Although this is probably acceptable for the purposes of the analysis in reference [54], the important physics of the interplay of sedimentation and depletion-induced flocculation is fundamentally non-equilibrium and dominated by the hydrodynamic interaction, and should be studied as such. In addition, all discussions of bidisperse sedimentation have concentrated on the batch-settling mode; the steady-state phase diagram of such systems has received no attention until the recent theoretical work of reference [59] which I shall describe in brief below. Before doing so let me summarize work on other aspects of bidisperse sedimentation.

6.2. *Settling speeds in two-component sedimentation*

There is a fairly extensive literature on the settling speeds of mixtures [99–101] which I review very briefly here for general interest and completeness. The emphasis in such studies is on the dependence of mean speed on large- and small-particle volume fractions and radius ratios, not on spatial structure or velocity fluctuations. These speed measurements are compared to Batchelor and Wen's theory [102] for dilute bidispersions, and good agreement is generally found. The respective roles played by large and small particles in determining the hindered settling function [24] depend on the regime of concentration studied. For total (small + large) volume fraction $\phi < 20\%$, large particles are mainly responsible for the hindrance, whereas for $\phi > 35\%$, the large particles are slowed down more, and the small ones less, compared to the monodisperse case. At large enough concentrations, size segregation is greatly suppressed and both species settle together, the large dragging the small [99]. The addition of small particles to a large-particle suspension was argued [100] to *reduce* the settling speed, for at least two reasons. (i) Particle-surface roughness was argued to promote small-particle adsorption to the large-particle

surfaces, thus increasing their friction and slowing down their sedimentation. (ii) As argued in reference [102], the small particles also increase the effective solvent viscosity faced by the large particles, which too slows down sedimentation. Davis and Hassen [103] studied the effect of polydispersity on the interface at the top of a sedimenting suspension. They found that the interface, which is extremely sharp in monodisperse suspensions, was made more diffuse by polydispersity. This points to a possible role of polydispersity in enhancing velocity fluctuations.

6.3. *Hydrodynamic instabilities in bidisperse settling*

Experiments on the sedimentation of bidisperse mixtures of particles with radii in the 10 to 100 μm range show intriguing spatial structures including vertical streaming columns [104]. Batchelor and van Rensburg [58] analysed such systems by writing down partial differential equations for the local volume fractions ϕ_1 and ϕ_2 of the two species of particles. The crucial and physically very plausible ingredient in their theory was that the local drift velocity $\mathbf{U}_i$, $i = 1, 2$ of each species of particle relative to the centre of mass depended on the local values of both ϕ_1 and ϕ_2. A linear instability with growth rate $\propto k$ at wavenumber k was found if the matrix $K_{ij} \equiv \mathbf{k}.\partial(\phi_i \mathbf{U}_i)^0/\partial\phi_j$, where the superscript 0 refers to the unperturbed, spatially uniform suspension, satisfied $(K_{11} - K_{22})^2 + 4K_{12}K_{21} < 0$. Hydrodynamic dispersion will control this instability at larger wavenumbers, but cannot alter its basic structure. The instability, since $\mathbf{U}_i^0$ is vertical, is with respect to modulations along the sedimentation direction, and cannot thus give rise to columnar structures. Batchelor and van Rensburg [58] argue that the instability in these dispersions is fundamentally with respect to perturbations with vertical wavenumbers, that even when they saw columns they were preceded by blobs, and that the column formation, when it does happen, is a secondary effect. It should be noted that the effect of long-range velocity fluctuations induced by concentration fluctuations (see section 4) are not taken into account in the analysis of reference [58], although we shall argue below that they could be very important, especially near an instability towards phase separation.

6.4. *Velocity fluctuations in bidisperse sedimentation*

In reference [105] the structure of velocity fluctuations in bidisperse sedimentation was measured in a batch-settling experiment. The study found four sedimentation zones—from top to bottom, a clear supernatant, a stratum of small particles, a mixed layer containing small (radius 200 μm) and large (400 μm) particles, and the sediment. Their findings could be rationalized by assigning two screening lengths (see section 4) for the two species. The motion of large particles through the small-particle zone seemed to affect the fluctuations in the velocity of the latter. These preliminary experiments clearly call for a detailed theory of the statistical mechanics of bidisperse suspensions. From the point of view presented in this review, it would be best if these experiments were performed in the fluidized bed geometry so that the statistical physics of the steady state could be sorted out before going on to the more complicated non-stationary problem of batch settling.

6.5. *Depletion, screening, and microphase separation in sedimentation?*

One limit in which the problem of two-component sedimentation might prove more tractable is that in which one of the particles is very small and Brownian. In that case it is reasonable to treat the small particles as providing an attractive

depletion interaction between the large ones. This could conceivably lead, in the absence of sedimentation, to a critical point [9], or at least to a situation where large-particle concentration fluctuations are greatly enhanced. When sedimentation, i.e. the local force–density fluctuations implied by the concentration fluctuations, is taken into account, the consequences for the velocity fluctuations are alarming. To take an extreme case, suppose the large particles were actually at a critical point of a gas–liquid condensation. In a mean-field description, their structure factor would be $S(k) = 1/(ka)^2$, where a is a length of order of the large-particle radius. The resulting velocity standard deviation $\sigma_U(L)$ at length scale L in a system with mean settling speed U would then scale, extending the Caflisch–Luke [16] idea (see section 4), as $U\phi^{1/2}(L/a)^{3/2}$. Worse, in a Stokesian approximation, the characteristic time scale would be $L/\sigma_U(L) \sim (a/U)(a/L\phi)^{1/2}$, suggesting that fluctations relax faster on longer length scales. I can think of only two ways out. *Either* the neglect of inertia is simply wrong beyond length scales where $\mathrm{Re}(L) \equiv \sigma_U(L)L/\nu$, the *fluctuation* Reynolds number in a system with kinematic viscosity ν, becomes large, *or* a screening analogous to that in reference [30] intervenes at a scale shorter than such a crossover scale. It is likely, as in the monodisperse case (see section 4.5.4), that both screened and unscreened phases can arise; the physics in at least the unscreened phase is likely to involve inertia in a significant way. Preliminary results [59] suggest the following scenario: as the system parameters are allowed to approach the range where a critical point would have occurred at thermal equilibrium, the (equilibrium) correlation length grows, and hence so does the static structure factor. However, at longer length scales, the screening mechanism [30] takes over, so that the small-wavenumber structure factor is suppressed. The result is a structure factor with a peak at an intermediate wavenumber for directions normal to gravity. This clearly raises the possibility of ordered, columnar structures at intermediate length scales, by a mechanism quite different from any discussed in references [58, 104]. There is also the intriguing possibility that analogues of the depletion interaction arise even in driven (and hence noisy) suspensions without *thermal* noise, in which case the ideas discussed in this section could be extended to non-Brownian systems.

7. Conclusion

This article has attempted to present the current state of understanding of steady-state sedimentation in a highly viscous fluid, from the point of view of a statistical physicist. It is hoped that the reader now sees the problem of dirt settling in a fluid as a challenging problem at the frontier of non-equilibrium statistical physics. The article has summarized progress on a few selected problems in sedimentation, which in turn is a subset of the large class of problems in which particles are driven through viscous fluids, by gravity, imposed shear, electrophoresis [9] and the motion of self-propelled organisms [106, 107]. It should be clear that this small subfield itself has a great many open problems, to which I hope some readers will be drawn.

References

[1] Einstein, A., 1906, *Ann. Phys.*, **19,** 289; 1926, *Investigations on the Theory of the Brownian Movement* (London: Methuen) (reprinted by Dover, New York, 1956).
[2] Langevin, P., 1908, *Comptes rendus*, **146,** 530.
[3] von Smoluchowskii, M., 1916, *Phys. Zeits.*, **17,** 557.

[4] CHANDRASEKHAR, S., 1943, *Rev. mod. Phys.*, **15,** 1; reprinted in Wax, N., 1954, *Selected Papers on Noise and Stochastic Processes* (New York: Dover).
[5] PERRIN, J., 1916, *Atoms* (London: Constable) (reprinted by Oxbow Press, Amherst, MA, USA, 1990).
[6] SOOD, A. K., 1991, *Solid State Physics*, Vol. 45, edited by H. Ehrenreich and D. Turnbull (New York: Academic Press), p. 1.
[7] See, e.g. PUSEY, P., and RAMASWAMY, S., 1997, *Theoretical Challenges in the Dynamics of Complex Fluids*, *Lectures in a NATO Advanced Study Institute Series*, edited by T. C. B. McLeish (Amsterdam: Kluwer); Hulin, J. P., Cazabat, A.-M., Guyon, E., and Carmona, F. (eds), 1990, *Hydrodynamics of Dispersed Media* (North-Holland/Elsevier).
[8] See, e.g. ACKERSON, B. J., and CLARK, N. A., 1984, *Phys. Rev.* A, **30,** 906; LAHIRI, R., and RAMASWAMY, S., 1994, *Phys. Rev. Lett.*, **73,** 1043; PALBERG, T., and WURTH, M., 1996, *J. Phys.* (*Paris*), **6,** 237.
[9] RUSSEL, W. B., SAVILLE, D. A., and SCHOWALTER, W. R., 1989, *Colloidal Dispersions* (Cambridge: Cambridge University Press).
[10] BLANC, R., and GUYON, E., 1991, *La Recherche*, **22,** 866.
[11] KYNCH, G. J., 1952, *Trans. Faraday Soc.*, **48,** 166.
[12] BRADY, J. F., and BOSSIS, G., 1988, *Annu. Rev. fluid Mech.*, **20,** 111.
[13] JÁNOSI, I. M., TEL, T., WOLF, D. E., and GALLAS, J. A. C., 1997, *Phys. Rev.* E, **56,** 2858.
[14] DE GROOT, S. R., and MAZUR, P., 1984, *Non-equilibrium Thermodynamics* (New York: Dover).
[15] XUE, J. Z., HERBOLZHEIMER, E., RUTGERS, M. A., RUSSEL, W. B., and CHAIKIM, P. M., 1992, *Phys. Rev. Lett.*, **69,** 1715.
[16] CAFLISCH, R. E., and LUKE, J. H. C., 1985, *Phys. Fluids*, **28,** 759.
[17] SEGRÈ, P. N., HERBOLZHEIMER, E., and CHAIKIN, P. M., 1997, *Phys. Rev. Lett.*, **79,** 2574.
[18] HINCH, E. J., 1988, *Disorder in Mixing*, edited by E. Guyon *et al.* (Dordrecht: Kluwer Academic).
[19] BATCHELOR, G. K., 1970, *J. fluid Mech.*, **41,** 545; 1972, *ibid.*, **52,** 245.
[20] TORY, E. M., KAMEL, M. T., and CHAN MAN FONG, C. F., 1992, *Powder Technol.*, **73,** 219.
[21] BRENNER, M. P., 1999, *Phys. Fluids*, **11,** 754.
[22] LEI, X., ACKERSON, B. J., and TONG, P., 2001, *Phys. Rev. Lett.*, **86,** 3300.
[23] KOGLIN, B., 1971, *Chem. Ing. Tech.*, **43,** 761, and other works by the same author cited in reference [20].
[24] HAM, J. M., and HOMSY, G. M., 1988, *Int. J. multiphase Flow*, **14,** 533.
[25] NICOLAI, H., and GUAZZELLI, E., 1995, *Phys. Fluids*, **7,** 3; NICOLAI, H., HERZHAFT, B., HINCH, E. J., OGER, L., and GUAZZELLI, E., 1995, *ibid.*, **7,** 12.
[26] COWAN, M. L., PAGE, J. H., and WEITZ, D. A., 2000, *Phys. Rev. Lett.*, **85,** 453.
[27] LADD, A. J. C., 1996, *Phys. Rev. Lett.*, **76,** 1392; 1997, *Phys. Fluids*, **9,** 491.
[28] ROUYER, F., MARTIN, J., and SALIN, D., 1999, *Phys. Rev. Lett.*, **83,** 1058; ROUYER, F., LHUILLIER, D., MARTIN, J., and SALIN, D., 2000, *Phys. Fluids*, **12,** 958.
[29] SEGRÈ, P., LIU, F., UMBANHOWAR, P., and WEITZ, D. A., 2001, *Nature*, **409,** 594.
[30] LEVINE, A., RAMASWAMY, S., FREY, E., and BRUINSMA, R., 1998, *Phys. Rev. Lett.*, **81,** 5944; 1999, *Structure and Dynamics of Materials in the Mesoscopic Domain*, edited by B. D. Kulkarni and Moti Lal (London: Imperial College Press & The Royal Society).
[31] KOCH, D. L., and SHAQFEH, E. S. G., 1991, *J. fluid Mech.*, **224,** 275.
[32] HALPERIN, B. I., and HOHENBERG, P. C., 1977, *Rev. mod. Phys.*, **49,** 435.
[33] MARTIN, P. C., PARODI, O., and PERSHAN, P. S., 1972, *Phys. Rev.* A, **6,** 2401.
[34] LANDAU, L. D., and LIFSHITZ, I. M., 1959, *Fluid Mechanics* (Oxford: Pergamon).
[35] TONG, P., and ACKERSON, B. J., 1998, *Phys. Rev.* E, **58,** 6931.
[36] RAMAKRISHNAN, T. V., and YUSSOUFF, M., 1979, *Phys. Rev.* B, **19,** 2775; RAMAKRISHNAN, T. V., 1984, *Pramana*, **22,** 365.
[37] RUTGERS, M. A., XUE, J.-Z., HERBOLZHEIMER, E., RUSSEL, W. B., and CHAIKIN, P. M., 1995, *Phys. Rev.* E, **51,** 4674.
[38] RUTGERS, M. A., 1995, PhD thesis, Princeton University, USA.

[39] See, e.g. BALENTS, L., MARCHETTI, M. C., and RADZIHOVSKY, L., 1998, *Phys. Rev.* B, **57,** 7705.
[40] LAHIRI, R., and RAMASWAMY, S., 1997, *Phys. Rev. Lett.*, **79,** 1150.
[41] LAHIRI, R., BARMA, M., and RAMASWAMY, S., 2000, *Phys. Rev.* E, **61,** 1648.
[42] RAMASWAMY, S., 1998, *Dynamics of Complex Fluids*, edited by M. J. Adams, R. A. Mashelkar, J. R. A. Pearson and A. R. Rennie (London: Imperial College Press & The Royal Society).
[43] CROWLEY, J. M., 1971, *J. fluid Mech.*, **45,** 151; 1976, *Phys. Fluids*, **19,** 1296.
[44] LANDAU, L. D., and LIFSHITZ, I. M., 1965, *Theory of Elasticity* (Oxford: Pergamon).
[45] SIMHA, R. A., and RAMASWAMY, S., 1999, *Phys. Rev. Lett.*, **83,** 3285.
[46] SCHMITTMANN, B., and ZIA, R. K. P., 1995, *Phase Transitions and Critical Phenomena*, Vol. 17, edited by C. Domb and J. L. Lebowitz (London: Academic Press).
[47] BRAY, A. J., 1994, *Adv. Phys.*, **43,** 357.
[48] SOLLICH, P., WARREN, P. B., and CATES, M. E., 2001, *Adv. Chem. Phys.*, **116,** 265.
[49] ASAKURA, S., and OOSAWA, F., 1954, *J. chem. Phys.*, **22,** 1255; 1958, *J. polymer Sci.*, **33,** 183.
[50] BIBEN, T., and HANSEN, J. P., 1991, *Phys. Rev. Lett.*, **66,** 2251.
[51] VRIJ, A., 1976, *Pure appl. Chem.*, **48,** 471.
[52] SANYAL, S., EASWAR, N., RAMASWAMY, S., and SOOD, A. K., 1992, *Europhys. Lett.*, **18,** 107.
[53] DINSMORE, A. D., YODH, A. G., and PINE, D. J., 1996, *Nature*, **383,** 239.
[54] CHU, X. L., NIKOLOV, A. D., and WASAN, D. T., 1996, *Chem. Eng. Comm.*, **150,** 123.
[55] BIBETTE, J., 1991, *J. colloid interface Sci.*, **147,** 474.
[56] WILLIAMS, W., BEUTLER, E., ERSLEV, A., and LICHTMAN, M., 1990, *Hematology*, 4th edition (New York: McGraw-Hill Inc.), p. 1588.
[57] BROOKS, D. E., 1995, *Biorheology* **32,** 103; Kobuchi, Y., *et al.*, 1988, *J. theor. Biol.*, **130,** 129.
[58] BATCHELOR, G. K., and JANSE VAN RENSBURG, W., 1986, *J. fluid Mech.*, **379,** 166.
[59] SIMHA, R. A., and RAMASWAMY, S., unpublished.
[60] HAPPEL, J., and BRENNER, H., 1965, *Low Reynolds Number Hydrodynamics* (Englewood Cliffs, NJ: Prentice Hall).
[61] STOKES, G. G., 1845, *Proc. Camb. Phil. Soc.*, **8,** 287; 1851, *ibid.*, **9,** 8.
[62] STIMSON, M., and JEFFERY, G. D., 1926, *Proc. R. Soc. London* A, **111,** 110; Goldman, A. J., Cox, R. J., and BRENNER, H., 1966, *Chem. Eng. Sci.*, **21,** 1151.
[63] BEENAKKER, C. W. J., VAN SAARLOOS, W., and MAZUR, P., 1984, *Physica* A, **127,** 451.
[64] SAFFMAN, P. G., 1973, *Stud. appl. Maths.*, **52,** 115.
[65] ADRIAN, R. J., 1991, *Annu. Rev. fluid Mech.*, **23,** 261.
[66] BERNE, B., and PECORA, R., 1990, *Dynamic Light Scattering: with Applications to Chemistry, Biology, and Physics* (Malabar, FL: Krieger).
[67] MARET, G., and WOLF, P. E., 1987, *Z. Phys. B*, **65,** 409; PINE, D. J., WEITZ, D. A., CHAIKIN, P. M., and HERBOLZHEIMER, E., 1991, *Phys. Rev. Lett.*, **60,** 1134; WEITZ, D. A., and PINE, D. J., 1992, *Dynamic Light Scattering*, edited by W. Brown (Oxford: Oxford University Press), p. 652.
[68] SMITH, T. N., 1968, *J. fluid Mech.*, **32,** 203.
[69] LADD, A. J. C., 1994, *J. fluid Mech.*, **271,** 285; 1994, *ibid.*, **271,** 311.
[70] KOCH, D. L., 1994, *Phys. Fluids*, **6,** 2894.
[71] BLAKE, J., 1971, *Proc. Camb. Phil. Soc.*, **70,** 303.
[72] LORENTZ, H. A., 1907, *Abhand. Theor. Phys.* (*Leipzig*), **1,** 23.
[73] DEBYE, P., and HÜCKEL, E., 1923, *Z. Phys.*, **24,** 185; see also the treatment in [74].
[74] CHAIKIN, P. M., and LUBENSKY, T. C., 1998, *Principles of Condensed Matter Physics* (New Delhi: Cambridge University Press).
[75] LADD, A. J. C., 1993, *Phys. Fluids* A, **5,** 199.
[76] MORI, H., and FUJISAKA, H., 1973, *Prog. Theor. Phys.*, **49,** 764.
[77] LEIGHTON, D., and ACRIVOS, A., 1987, *J. fluid Mech.*, **177,** 109; 1987, *ibid.*, **181,** 415.
[78] HAYOT, F., JAYAPRAKASH, C., and PANDIT, R., 1993, *Phys. Rev. Lett.*, **71,** 1.
[79] MA, S. K., 1976, *Modern Theory of Critical Phenomena* (Reading MA: Benjamin).
[80] FORSTER, D., NELSON, D. R., and STEPHEN, M. J., 1977, *Phys. Rev.* A, **16,** 732.
[81] GRINSTEIN, G., LEE, P. A., and SACHDEV, S., 1990, *Phys. Rev. Lett.*, **64,** 1927.

[82] FORSTER, D., 1980, *Hydrodynamic Fluctuations, Broken Symmetry, and Correlation Functions* (Reading: Benjamin).
[83] CHANDRASEKHAR, S., 1981, *Hydrodynamic and Hydromagnetic Stability* (New York: Dover).
[84] KRAICHNAN, R., 1962, *Phys. Fluids*, **5,** 1374.
[85] PRIESTLEY, C. H. B., 1959, *Turbulent Transfer in the Lower Atmosphere* (Chicago: University of Chicago Press).
[86] PAULIN, S. E., and ACKERSON, B. J., 1990, *Phys. Rev. Lett.*, **64,** 2663.
[87] LAHIRI, R., and RAMASWAMY, S., 1998, cond-mat/9811052.
[88] DAS, D., BASU, A., BARMA, M., and RAMASWAMY, S., 2001, *Phys. Rev.* E, accepted.
[89] RAMASWAMY, S. BARMA, M. DAS, D., and BASU, A., 2000, *Proceedings of the Meeting on Slow Dynamics and Freezing*, Jawaharlal Nehru University, March (to be published in *Phase Transitions*).
[90] BARMA, M., and RAMASWAMY, S., 2001, *Turkish J. Phys.*, **24,** 235.
[91] EVANS, M. R., 2000, cond-mat/0007293.
[92] BASU, A., BHATTACHARJEE, J. K., and RAMASWAMY, S., 1999, *Eur. Phys. J.* B, **9,** 725.
[93] ERTAŞ, D., and KARDAR, M., 1992, *Phys. Rev. Lett.*, **69,** 929; 1993, *Phys. Rev.* E, **48,** 1228; BOUCHAUD, J.-P., BOUCHAUD, E., LAPASSET, G., and PLANÈS, J., 1993, *Phys. Rev. Lett.*, **71,** 2240; BARABÁSI, A.-L., 1992, *Phys. Rev.* A, **46,** R2977.
[94] DAS, D., and BARMA, M., 2000, *Phys. Rev. Lett.*, **85,** 1602.
[95] LANDAU, L. D., and LIFSHITZ, E. M., 1969, *Statistical Physics* (Reading, MA: Addison-Wesley).
[96] EVANS, M. R., KAFRI, Y., KODUVELY, H. M., and MUKAMEL, D., 1998, *Phys. Rev. Lett.*, **80,** 425; 1998, *Phys. Rev.* E, **58,** 2764.
[97] BASKURT, O. K., TEMIZ, A., and MEISELMAN, H. J., 1997, *J. Lab. clin. Med.*, **130,** 183.
[98] ADAMS, M., and FRADEN, S., 1998, *Biophys. J.*, **74,** 669.
[99] HOYOS, M., BACRI, J. P., MARTIN, J., and SALIN, D., 1994, *Phys. Fluids*, **6,** 3809.
[100] THIES-WEENIE, D. M. E., PHILIPSE, A. P., and LEKKERKERKER, H. N. W., 1996, *J. coll. interf. Sci.*, **177,** 427.
[101] AL-NAAFA, M. A., and SAMI SELIM, M., 1992, *AIChE J.*, **38,** 1618.
[102] BATCHELOR, G. K., 1982, *J. fluid Mech.*, **119,** 577; BATCHELOR, G. K., and WEN, C.-S., 1982, *ibid.*, **124,** 495.
[103] DAVIS, R. H., and HASSEN, M. A., 1988, *J. fluid Mech.*, **196,** 107.
[104] FESSAS, Y. P., and WEILAND, R. E., 1981, *AIChE J.*, **27,** 588.
[105] PEYSSON, Y., and GUAZZELLI, E., 1999, *Phys. Fluids*, **11,** 1953.
[106] PEDLEY, T. J., and KESSLER, J. O., 1992, *Annu. Rev. fluid Mech.*, **24,** 313.
[107] WU, X. L., and LIBCHABER, A., 2000, *Phys. Rev. Lett.*, **84,** 3017.